Journal of Materials Chemistry C

ROYAL SOCIETY OF CHEMISTRY

REVIEW

View Article Online
View Journal | View Issue

Cite this: J. Mater. Chem. C, 2020, 8, 10136

Nanostructured conducting polymers and their composites: synthesis methodologies, morphologies and applications

Yu Xue,[a] Shuai Chen, *[ab] Jiarui Yu,[a] Benjamin R. Bunes,[c] Zexu Xue,[a] Jingkun Xu,[a] Baoyang Lu *[ad] and Ling Zang *[b]

Received 2nd May 2020,
Accepted 26th June 2020

DOI: 10.1039/d0tc02152k

rsc.li/materials-c

Nanostructured conducting polymers (NCPs) have been extensively studied and widely applied in state-of-the-art technologies over the past few decades because they simultaneously offer the photoelectric features and processing advantages of polymeric conductors and the nano-size effect of nanomaterials. With rational design and synthesis, NCPs with controllable morphologies and physicochemical properties can exhibit fascinating electrical, optical, mechanical, and biological properties. In this review, we describe in detail the synthetic methodology and the relationship of morphology–property of NCPs as well as their recent advances in biotherapy, biosensing, microwave absorbers for electromagnetic shielding, and various energy storage/conversion/saving devices. And last, since this field contains many immense scopes for exploration and development, we bring new insights along with a brief summary.

1. Introduction

Research on conducting polymers (CPs) is one of the hotspots in the field of materials due to their special polymeric structures and fascinating electrical, optical, mechanical, and biological properties; hence, they have been widely applied in many fields such as biotherapy, chemical/biological sensors, photo-/electrocatalysis, energy storage and conversion devices, electromagnetic shielding, and so on.[1–3] In comparison to conventional semiconductors, CPs possess unique bonding structures along the polymer backbones, consisting of alternating double (π) and

[a] Flexible Electronics Innovation Institute, Jiangxi Science & Technology Normal University, Nanchang 330013, Jiangxi, China
[b] Nano Institute of Utah, and Department of Materials Science and Engineering, University of Utah, Salt Lake City, UT 84112, USA. E-mail: shuai.chen@utah.edu, lzang@eng.utah.edu; Fax: +1-801-581-4816; Tel: +1-801-809-7987
[c] Vaporsens Inc., 615 Arapeen Drive, Suite 102, Salt Lake City, UT 84112, USA
[d] Department of Mechanical Engineering, Massachusetts Institute of Technology, Cambridge, MA 02139, USA. E-mail: luby@mit.edu

Yu Xue

Yu Xue received his Bachelor's Degree in Applied Chemistry in Beihua University, P. R. China. He is currently a master student under the supervision of Prof. Shuai Chen and Prof. Baoyang Lu in Jiangxi Science & Technology Normal University, P. R. China. His main research fields include the synthesis of conducting polymers as well as their applications in electrochromic devices.

Shuai Chen

Shuai Chen is a professor hired by Jiangxi Science & Technology Normal University, P. R. China. He earned his PhD degree (2015) in materials physics and chemistry from University of Chinese Academy of Sciences, and since 2018 is a postdoctoral fellow with Prof. Ling Zang at University of Utah. His current research emphasizes the design and fabrication of functional nanostructured semiconductors and nanocomposites for sensors and energy-transfer optoelectronics, as well as intrinsic conducting polymers with flexible electronic applications.

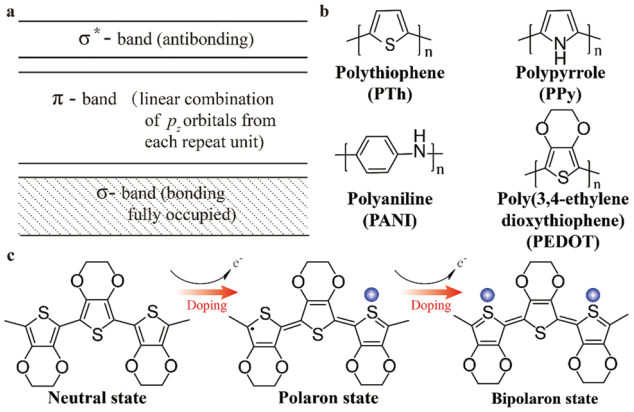

Fig. 1 (a) Schematic band diagram for CPs. (b) Chemical structures of commonly used CPs including polythiophene (PTh), polypyrrole (PPy), and polyaniline (PANI), poly(3,4-ethylenedioxythiophene) (PEDOT). (c) Conducting mechanism of PEDOT.

single (σ) bonds (Fig. 1a), which endow them semiconducting properties.[2] Once doped, the π-systems accommodate negative or positive charges that can pair with the dopants to form polarons, and can further be oxidized to bipolarons (supporting the transport of both holes and electrons). As shown in Fig. 1b, there are four typical categories of CPs including polyaniline (PANI), polypyrrole (PPy), polythiophene (PTh), and poly(3,4-ethylenedioxythiophene) (PEDOT).[2–4] The conductive mechanism exemplified by PEDOT is illustrated in Fig. 1c.

However, conventional CPs with amorphous bulk-phase are usually fall short in terms of electrical, optical and biological properties, thus have to confine their dimensions.[1] In comparison to bulk CPs, nanostructured CPs (NCPs) provide superior electrical conductivity, higher carrier mobility, special electrochemical activity, improved optical properties and good biocompatibility, *etc.*, owing to their well-defined nanostructures and larger surface areas.[1,5] Simultaneously, NCPs can be manufactured into diverse nanostructures from zero-dimensional (0D) nanoparticles, one-dimensional (1D) nanowires, two-dimensional (2D) nanofilms to three-dimensional (3D) network nanostructures to satisfy special requirements from various fields.[5,6] In addition, these hybrid NCPs can retain the functionalities from individual components as well as synergistic effects when they are integrated with other functional materials such as metals, metal oxides, carbon materials, non-conducting polymers, and so on.[1,5] The morphology and structure of NCPs exert significant effects on their conductivity and physicochemical efficiency, thus tremendous endeavors have been devoted to adjust their

Jiarui Yu

Jiarui Yu graduated in the major of Pharmaceutical Engineering from Jingchu University of Technology, P. R. China, and now is a master's student under the supervision of Prof. Shuai Chen in Jiangxi Science & Technology Normal University. She focuses on exploring self-healing thin-films of intrinsic conducting polymers as well as their uses in organic electronic devices.

Benjamin R. Bunes

Benjamin R. Bunes is the Director of Research and Development of Vaporsens, Inc. He holds a Ph. D. in Materials Science and Engineering from the University of Utah. He has been involved in research surrounding nanotechnology/nanomaterials for thirteen years, with the past ten years focused on nanomaterial sensors for chemical detection. He was previously a NASA Space Technology Research Fellow and ASEE/NSF Small Business Postdoctoral Research Diversity Fellow.

Zexu Xue

Zexu Xue has a Bachelor degree in Chemical Engineering and Technology from Liaocheng University, P. R. China. He is currently pursuing master under the supervision of Prof. Shuai Chen at Jiangxi Science & Technology Normal University, P. R. China. He mainly works on the development of organic semiconductor one-dimensional nanostructured materials.

Jingkun Xu

Jingkun Xu is a full professor at Jiangxi Science and Technology Normal University in China. He received his PhD degree in Polymer Chemistry and Physics from Tsinghua University in 2003. His current research interests include synthesis of conducting polymers and their applications for thermoelectrics, electrochromics, fuel cells, sensors, and supercapacitors.

surface area (*e.g. via* porous structure), phase, lattice fringes and patters in order to meet the different requirements from various aspects. For example, NCPs with porous structure can incorporate multiple chemical functionalities into the porous framework or at the open site of pores. Such porous structure endows increasing surface area, providing more electrochemically active sites and electrolyte–electrode interface for ion storage, thus enhancing their specific capacity or sensing capability. In brief, there are three main factors to facilitate the rapid development of NCPs and their nanocomposites over recent few years. One important contributor is a deeper understanding of the mechanism of the charge transfer and transport processes as well as the interface properties among NCPs and corresponding composites and devices.[5,6] The second driver is emerging processing and manufacturing technologies that have accelerated and simplified the fabrication of NCPs.[1,5,6] Another is ascribed to the gradually progressive preparation and performance measurement technologies that enable diverse applications.[5] In contrast to the satisfying applications of NCPs in biological, optoelectronic, and energy-related fields,[1,5–9] several reviews have been published previously about their material synthesis and physicochemical studies.[6–12] Since a deep understanding for fabrication strategies and morphology control as well as structure–properties relationship is highly important for accelerating the development of NCPs into high-performance products.

For that purpose, the fabrication strategies of NCP materials as well as the integrated techniques to forming their nanocomposites are comprehensively summarized in this review. The morphological structures and physicochemical properties of NCPs and hybrid nanomaterials are emphatically discussed, aiming to deepen the understanding in the relationships between them. Thereafter, their exciting applications in biotherapy, biosensing, microwave absorbers for electromagnetic shielding, and energy storage/conversion/saving devices are discussed. Lastly, we provide a brief summary and perspective regarding the opportunities and challenges within this field for promoting its future development.

2. Synthesis methodology of NCPs

Understanding the processes for growth and assembly is vital for fabricating targeted polymers with target nanostructures and sizes.[1] In general, the fabrication method of nanomaterials like NCPs can be classified into two categories, bottom-up and top-down approaches. The main difference between the two methods lies in the process of preparing NCPs.[13] In the bottom-up approach, NCPs are prepared from monomers, which allows for more control of reaction kinetics and growth in size, as well as self-assembly into more complex structures. In comparison, bottom-up fabrication often makes use of deposition techniques (*e.g.*, chemical vapor deposition) and surface supported molecular self-assembly processes (*e.g.*, self-assembled monolayers).[13] With top-down approach, the components of NCPs are from some bulk resources in liquid or solid state.[13] The assembly of nanostructure in top-down approach can be realized through lithographic techniques (namely physical top-down) or chemical vapor mediated processes (chemical top-down).[13] In this review, the fabrication of NCPs will be focused more on the bottom-up approach.

During the polymerization process, their properties can be influenced by changing the concentrations of monomers and dopants, and different polymerization methods like chemically oxidative and electrochemical polymerization. Parameters such as the concentration of monomer, the type of oxidant, reaction time and temperature, the characteristics of template also need to be emphasized in the synthesized processes.[1,6,12] As a result, structures and physiochemical properties of polymers can be tuned by controlling the synthetic conditions.[12] In short, the physiochemical properties including electrical and optical features and crystallinity of NCPs depend on the synthesis methods or confined conditions.[12] The final properties of NCPs could be influenced *via* subtle contributions of multi-length scale factors such as trace impurities, conformation, nanostructure and gross morphology.[1,5,6,12]

2.1 Hard-templating

Hard-templating is a common and effective tool for preparing NCPs with regular structure such as nanospheres, nanowires,

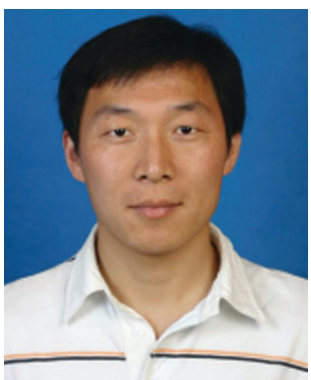

Baoyang Lu

Baoyang Lu is a full professor at Jiangxi Science & Technology Normal University in China. After receiving his PhD in Materials Science and Engineering from Shandong University, he worked as a postdoctoral fellow in Department of Mechanical Engineering at Massachusetts Institute of Technology (MIT) for three years. His current research interests include the design and synthesis of novel conjugated polymer-based molecular systems, and their fabrication technology and applications towards organic electronics and bioelectronics.

Ling Zang

Ling Zang is a professor at University of Utah, affiliated with Department of Materials Science and Engineering, and Nano Institute of Utah. He received his B.S. in physical chemistry from Tsinghua University and PhD in chemistry from the Chinese Academy of Sciences. His current research focuses on nanoscale imaging and molecular probing, organic semiconductors and nanostructures, optoelectronic sensors and nanodevices, with the long-term goal to achieve real applications in the areas of national security, health monitoring, renewable energy, and clean environment.

and nanotubes.[6] This process can be divided into three main steps: (1) infiltration or adsorption of the raw materials onto the surfaces or into interstitial voids in the templates, (2) *in situ* polymerization or solidification of the distributed raw materials, and (3) finally removal of the templates.[12,14] Templates are generally comprised of track-etched membranes, silica nanomaterials, anodic aluminum oxide (AAO), or other non-conductive polymer nanomaterials (*e.g.*, polydimethylsiloxane and block copolymers). They usually form porous cylinders or hollow structures; thus, the diameter of the nanomaterials is controlled by size of the pores in the template whereas the length and thickness of the nanostructures is usually adjusted by changing polymerization conditions or the concentration of monomers.[15,16] Therefore, these are two potential extreme modes for growing NCPs in hard-template. The first possibility is the formation of nanowires at a sufficient monomer supply and a slow reaction rate.[14] In this case, monomers can be slowly diffused into template and fill it, thus tends to form nanowires. The other possibility is the formation of nanotubes at an insufficient monomer supply and a fast reaction rate.[15] In this case, monomers are rapidly diffused from bulk solution and polymerized at the pore wall because of the interaction of polymer and wall surface. Above theory was further updated in the work of Xue *et al.*, and they found that single crystal PPy nanotube arrays can grow on the inside of the AAO template by changing the temperature of template.[17] They employ a micro-cold-wall vapor phase deposition technique to prepare PPy nanotubes in a low concentration of monomer solution. In this process, CPs prefer to grow orderly when the temperature is low enough, which is similar to the growth of ice on a cold surface. Thus, the structure of NCPs can be confined by adjusting the concentration of monomer, polymerization rate, and the temperature of the template.

However, there are some disadvantages for using conventional sacrificial templates. For example, the final morphology of NCPs can be influenced by the form and shape of the conducting base electrode in sacrificial template like using AAO template. Moreover, their nanostructure are usually presented in collapsed and aggregated states along with the removal of AAO template, owing to the strong surface tension between NCPs and liquid during solvent evaporation.[15,18] Therefore, how to maintain the integrity of NCPs is vital when without the support from templates.

Recent studies showed that TiO_2 nanotube (TNTs) as templates prefer to form CPs with stable network structure, owing to intrinsic semiconducting properties of TNTs.[15] Different from other types of templates, TNTs itself can serve as conducting base electrode, and the monomer can be electropolymerized inside the TNT templates. Thus, TNT templates do not require the deposition of any base electrode layer for polymer growth, which can guarantee the integrality of NCPs when the supporting templates are removed. Afterwards, Lee *et al.*, proposed the mechanism of nucleation and growth of PTh in TNTs (Fig. 2).[15] The formation of nanofibers is believed to follow a three-dimensional instantaneous nucleation and growth mode, indicating that the growth of CPs occurs in the existing sites rather than new polymerization sites. The formation of the initial nuclei occurs by the precipitation of oligomeric chains on the growth surface once they reach a chain length at which they are insoluble. Thus, the solubility of thiophene monomers (and subsequent oligomers) at the electrode–solution interface is crucial for achieving an efficient polymerization. The hollow TNTs provide a higher surface energy, thus it is likely that the nucleation and growth of subsequent nanofibers are mostly initiated from the bottom-most region of the TNTs. As a result, the TNTs provide an appropriate framework for PTh nanofibers to grow and extruded from the nanotubes during polymerization.

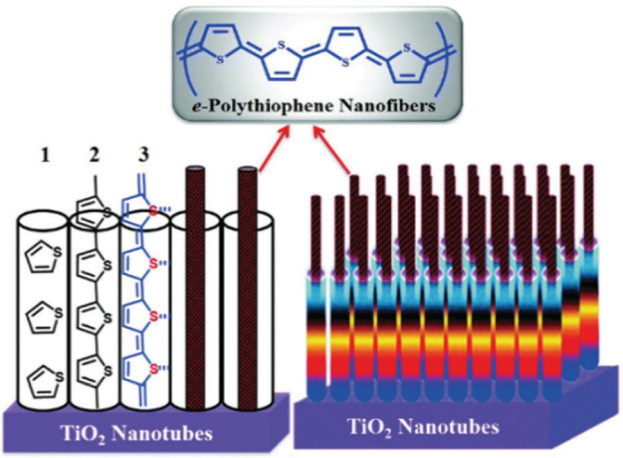

Fig. 2 Schematic preparation of 1D PTh nanofibers with controllable size by using TiO_2 nanotubes as templates. Reprinted with permission from ref. 15. Copyright 2017 Royal Society of Chemistry.

Although above TNTs template can control NCPs with steady structure, the preparation of TNTs is complicated and expensive. Thus, a low-cost and accessible hard-template is reliable for the larger-scale production of NCPs, which may require a change in the type of templates. For example, Park *et al.* synthesized pure 2D PANI nanosheets using ice as a removable hard template, as presented in Fig. 3.[19] Using ice as a template effectively restricted the growth of polymer nanofilms, which is ascribed to the unique advantage of ice surfaces, offering low potential

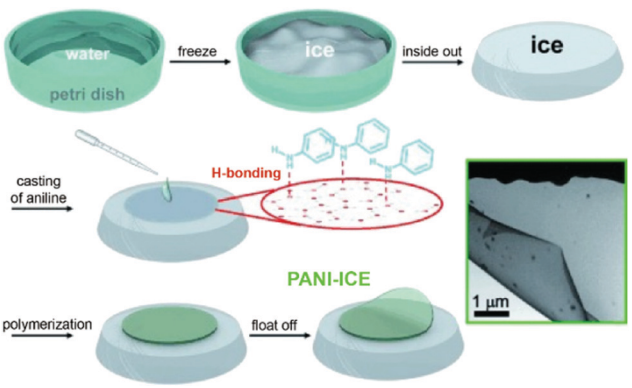

Fig. 3 The synthetic procedures for 2D PANI nanosheets on ice surfaces. Reprinted with permission from ref. 19. Copyright 2015 Wiley-VCH.

energy and quasi-ordered dangling –OH groups. Moreover, the simple template removal process (dissolution) also ensures the integrity and continuity of the film.

As a result, the hard-templating method can be regarded as an effective route to synthesize CP with regular structures like nanofibrils and nanotubes and the homogeneity, length, and diameter for the polymer fibers/tubes can be controlled by an appropriate choice of the template.[5,6,12] However, the preparation of NCPs with complex nanostructures is difficult by using the hard-template approach because of the limited types of template structures that are available.[12] Thus, other preparation methods can be selected, such as soft-templating.

2.2 Soft-templating

The soft-template methods generally use surfactants, colloidal particles and structure-directing molecule to form micelles, which in turn can confine the growth of CPs in dimensional size of nanometers, thus forming nanomaterials.[6] Compared to hard-templating approach, this approach is relatively simple and suitable for synthesizing NCPs in large scale.[6,12] With this approach, super-molecular structures have been achieved through self-assembly driven by hydrogen bonding, π–π stacking interactions, van der Waals forces, and electrostatic interaction.[6,12] The nanostructured morphology and size of NCPs thus grown are strongly dependent on the polymerization conditions, such as dopant and monomer properties, concentrations of dopant, monomer and oxidant, molar ratio of dopant and oxidant to monomer, reaction temperature, the nature of template used, *etc.*[12,18] Adjustment of these reaction parameters can be used as a simple approach to control the morphology and size of the nanostructures grown therein. For example, 1D NCPs (*e.g.*, nanowires in widths of 25–85 nm) can be prepared by using the surfactant templates with long alkyl chains such as cetyltrimethylammonium bromide (CTAB) or decyltrimethylammonium bromide (DTAB). In comparison, octyltrimethylammonium bromide (OTAB) or nonionic surfactants with shorter chains are often used to produce non-1D nanostructures, which is mostly due to the different role played by the short alkyl chains. All the surfactants that are used the most commonly as soft-template, contain a hydrophilic "head" and a long hydrophobic "tail" (mainly alkyl chain). Under the concerted intermolecular interactions, these surfactants form nanotube structure that can be used as a template to control the growth of NCPs. On the contrary, the structurally adjustable soft-template might properly provide a great chance to prepare complex 3D nanostructure, which is not achievable using the hard template method.[12] For example, Zhu *et al.* reported a novel hollow nanospheres of PANI with mesoporous, brain-like, convex-fold shell structures (Fig. 4a and b) *via* a micelle-mediated phase transfer method, using perfluorooctanoic acid/aniline as a soft template.[20] Accordingly, the growth mechanism is elucidated in Fig. 4c. Such complex nanostructures were difficult prepared by hard-template.

In addition, the morphology and properties of the NCPs can be controlled by varying the soft template materials and the synthesis conditions, such as the type of static surfactant. For

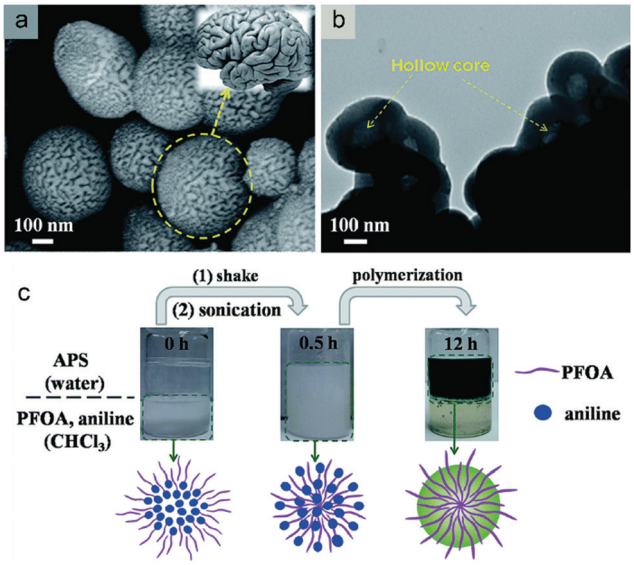

Fig. 4 (a) The magnification of the brain-like surface of PANI spheres, inset: photograph of human brain structures. (b) TEM image of the hollow PANI spheres. (c) Photos of polymerization processes *via* the micelle-mediated phase transfer method. Reprinted with permission from ref. 20. Copyright 2015 Royal Society of Chemistry.

example, Guo *et al.* reported a strategy of controlling the nanostructure of PANI by changing a static surfactant system at room temperature in a minimal acid environment.[21] A series of morphologies including spheres, roses, cloud-like and rhombic plates, layered flowers, columns, blocks, and dendrites were obtained by changing the types of surfactant.[21]

However, there are few strategies to fabricate nanomaterials with regular structures, especially planar nanofilms by soft-template method, owing to the lack of growth-driving force along two dimensions. Later, some researches indicated that the constraints of the growth space in the 2D orientation are a promising avenue for developing of 2D nanofilms. Jin *et al.* prepared PPy nanosheets by using a soft 2D template system composed of hundred-nanometer-thick water/ethanol mixed layers sandwiched to restrict the growth of PPy.[22] The resulting PPy nanofilms present a uniform thickness as thin as 3.8 nm and large dimensions (>2 μm^2). Thus, by means of the space limitation *via* molecular template can ensure the thickness of the film. In addition, a molecularly thick film could achieve a higher degree of crystallinity and an ordered interchain arrangement, which is advantageous for its macroscopic performances, especially electrical conductivity.

No extra processes are needed to prepare the sacrificial templates and the template-removal steps are not needed in the soft-template route. It also provides well-defined dynamic channels to obtain NCPs. However, poor stability of soft templates and difficultly in controlling the final morphology of the NCPs are challenging. There are some necessary problems which should be emphasized: the discharged waste water from soft template; some templates, such as lipid, DNA, tobacco mosaic virus, heparin, sodium alginate, are too expensive to be suitable for commercial production of NCPs.[12]

2.3 Electrospinning

Electrospinning is a promising method to fabricate long polymer nanofibers without using a template.[23,24] In this process, in general, a high electrical field is applied between a polymer fluid contained in a glass syringe with a capillary tip and a metallic collection screen. When the applied field reaches a critical value, the charge overcomes the surface tension of the deformed drop of the suspended polymer solution from the syringe tip and a jet is produced.[6,12,23,24] The electrically charged jet stretches during its passage to the collection screen.[6,12,23] Dry fibers are accumulated on the surface of the collection screen, resulting in a nonwoven mesh of nano-diameter fibers.[12]

The morphology and diameter of the fibers are a function of preparation parameters, such as the applied voltage, solution concentration, polymer molecular weight, solution surface tension, dielectric constant of the solvent, and solution conductivity.[6,12] In comparison to nanofibers prepared by hard and soft-template methods, electrospun nanofibers possess special characteristics, such as high aspect ratio, high surface to volume ratio, controlled length, pore size and superior mechanical properties.[6,23] However, the preparation of pure CP nanofibers is difficult by this method, owing to the insolubility of conventional CPs in routine aqueous and organic solution, such as PTh.[6,12] Some non-conducting polymers or chemicals (*e.g.*, plasma electrolytic oxidation, PEO) are usually added to assist with the formation of nanofibers, but may reduce conductivity and the physical and chemical properties of the fibers are usually altered.[25,26] To address this problem, electrospun polymer fibers can be used as template to prepare tubular materials with controlled dimensions. In this method, the electrospun polymer nanofibers are used as the template and CPs are then coated on the surface of the core fibers by *in situ* deposition polymerization from a solution containing monomer and oxidant.[12] This method can not only be used to produce coaxial CPs nanofibers, but also tubular CPs after dissolving the core polymer.[12,25]

In recent reports, modified methods are used to enrich electrical and biological performance. For example, Irani *et al.* presented a biocompatible PANI/polyacrylonitrile scaffold synthesized by modifying the electrospinning fiber with a non-thermal oxygen plasma.[27] In addition, Radacsi *et al.* reported a spontaneous formation of nanoparticles on the surface of smooth electrospun nanofibers containing polyvinylpyrrolidone or polyvinyl alcohol, and a small amount of emeraldine base PANI.[28] The spontaneous formation process of pretzel-stick-like composite structures consisting of nanoparticle-decorated nanofibers by electrospinning is shown in Fig. 5. The presence of nanoparticles on the fiber surface yielded composites with increased surface area of exposed electrolyte, which ultimately enhanced electrocatalytic performance.

2.4 Interfacial polymerization

CPs with 1D and 2D nanostructures can be formed in bulk by one-step aqueous/organic interfacial polymerization.[29] Different from conventional aqueous phase synthesis, the interfacial approach is performed in an immiscible organic/aqueous biphasic system to enable the initiation and propagation of the polymerization reaction with fewer nucleation sites.[5,29] It is a template-free approach, using high local concentrations of both monomer and dopant anions at the liquid–liquid interface to promote the formation of monomer-anion aggregates.[5,29] It allows for synthesis of high surface areas of NCPs or membrane layers with electrochemical properties. NCPs are established at the interface, and rapidly diffused into the aqueous phase, leaving the interface available for further reaction.[29] The polymerization rate of NCPs at this interface is regulated by varying factors, including the concentrations of the oxidant and monomer at the interface, their replenishment rate, and physical constraints regarding the physical mixing of the two chemical species.[29] Meanwhile, the type of obtained nanostructure depends on the organic solvents, acid dopants, the reaction time, and the concentration of monomer and oxidant.[12,29] For example, the length of PANI nanofibers was found to increase with acid strength.[12,29]

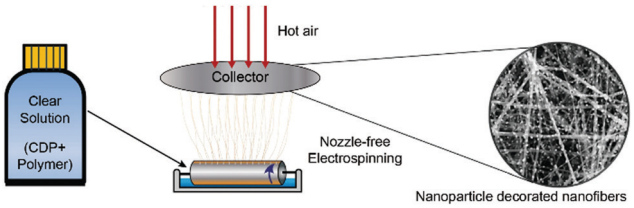

Fig. 5 The nanoparticle-decorated nanofibres are fabricated from a clear solution in a single step, containing dissolved caesium dihydrogen phosphate and polymers. Reprinted with permission from ref. 28. Copyright 2018 Nature Publishing Group.

As a result, this method is advantageous to prepare NCPs for the following reasons: (1) both the synthesis and purification are performed without a template, (2) the synthesis with an acceptable yield is easily scalable and re-producible, and (3) the nanofibers are readily dispersed in water, which could facilitate environmentally friendly processes and biological applications.[12,29] Future research on NCPs prepared *via* interfacial polymerization might focus on composites and covalent attachment of the polymers to a substrate or layer.[29]

2.5 Vapor-phase-polymerization

Vapor-phase polymerization (VPP) is a simple, fast, and cheap way to create conducting thin films with excellent quality.[30] Generally, VPP enables CPs with long conjugated degrees and high conductivity. In this procedure, a substrate is coated with an oxidant and placed in a heated chamber containing the appropriate monomer; the polymerization reaction takes place at a temperature above the monomer's melting point.[30] Monomer vapor in the chamber then condenses on the substrate where it is oxidized to form polymer chains. In fact, this process is a practical implementation of the oxidative polymerization method, where the oxidant (in solution) and monomer (as a vapor) come into intimate contact with the liquid–vapor interface.[30] During this process, polymerization occurs at the liquid–vapor interface created by the casting of an oxidant solution to the desired substrate which is subsequently exposed to the

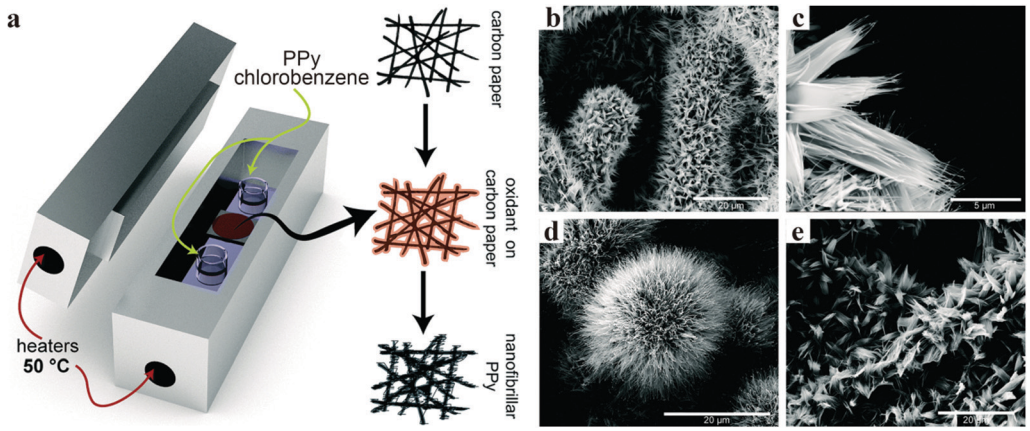

Fig. 6 (a) A schematic of evaporative vapour phase polymerization. (b) Scanning electron micrographs of unwashed PPy after vapour phase polymerization onto a hard carbon paper substrate. (c) High resolution SEM of nanoribbons of polypyrrole fanning out into nanofibers. (d) Droplets of oxidant serve as nucleation sites during polymerization and lead to radially symmetric rambutan shaped PPy. (e) Upon washing in 6 M HCl and methanol, the fibers relax yet remain separated. Reprinted with permission from ref. 32. Copyright 2017 Royal Society of Chemistry.

monomer vapor.[30,31] This technique has the advantages of the simplicity of procedure and the varieties of substrates and monomers that can be employed. VPP can synthesize soluble and insoluble polymers on various substrates; the substrate itself can be initially over-coated by an oxidant solution, and the precursor monomer can be vaporized.[30–32] The ease with which both monomer and oxidant can be used to manipulate polymer properties is a major advantage over other polymerization methods. However, this technique is rarely used in the preparation of nanostructured materials.

Recently, D'Arcy *et al.* reported a nanofibrillar PPy resembling nanobrushes by low-temperature evaporative VPP without the use of hard templates.[32] In this process, liquid oxidant is placed on the surface of the hard carbon paper and pyrrole is polymerized at 50 °C, thus PPy conformally coat on the surface of carbon papers (Fig. 6a). The different morphology of unwashed PPy are presented in Fig. 6b–e. The carbon paper itself has no spherical surface features, suggesting that microdroplets of oxidant solution can serve as templates for nanofiber nucleation. Thus, the self-assembly of nanofibrillar PPy described herein requires no hard templates and can be deposited directly onto a current collector, reducing the need for arduous and costly post-processing and template removal.

In addition, Kolodziejczyk *et al.* reported NCPs with a wall-like structure by the VPP method.[33] It is worth noting that the resulted nano-walls on the film surface increased the capacitance of the coating up to 3.4 times because the presence of nano-walls drastically increases the redox capacity of the film in accordance with a three-fold increase in surface area.[33]

2.6 Electrochemical approaches

Electrochemical polymerization is reliable for yielding electrode-type CPs, thus their thickness and morphology can be easy controlled by the deposition charge and rate. This approach is absence of an extra catalyst and the direct grafting of doped CPs onto the electrode surface. However, CPs usually have an irregular cauliflower-like morphology instead of nanostructure by individual electrochemical polymerization.[34] Thus, in order to obtain nanostructure, a template is needed to combine the structure and dimension of CPs. Overall, to select the suitable potential regime, concentration of monomers and category of templates are crucial for preparing NCPs, which have major effects on the deposition kinetics and subsequent further growth.

In order to get rid of templates, many efforts have been attempted. CP nanowire electrochemically polymerized and assembled onto two biased electrodes (anode and cathode) immersed in aqueous monomer solutions. The essence of this method is an electrode-wire-electrode or electrode-wire-target assembly.[6] For instance, CP nanowires are prepared by an electro-deposition within channels between two electrodes on the surface of silicon wafers. By using this way, Chouvy *et al.* prepared oriented PPy nanowires and found the diameter and the length of the nanowires can be increased when the solution contained a high concentration of weak-acid anions and a low concentration of non-acidic anions.[34] Since electrochemical polymerization is a shared and controlled method for preparing CPs and their nanostructures, electro-deposition within channels between two electrodes has received attention in fabricating molecule devices.[6,34,35]

2.7 Solvent evaporative self-assembly

Solvent evaporative self-assembly has been used to prepare CP with 1D nanostructure, but usually requires the polymers with amphipathicity between branched chain and conjugated chain. Poly-3-hexylthiophene (P3HT), as a typical amphipathic conjugated polymer, is extensively used in the preparation of organic electronics, and its nanostructures have been produced by template and other methods, especially solvent evaporative self-assembly, which is more conducive to preparing crystalline P3HT. Jung *et al.* reported a simple and facile one-pot strategy for fabricating uniform, large-area organic semiconducting thin films without complex processing.[36] During the solvent evaporation of floating P3HT solution on a water substrate,

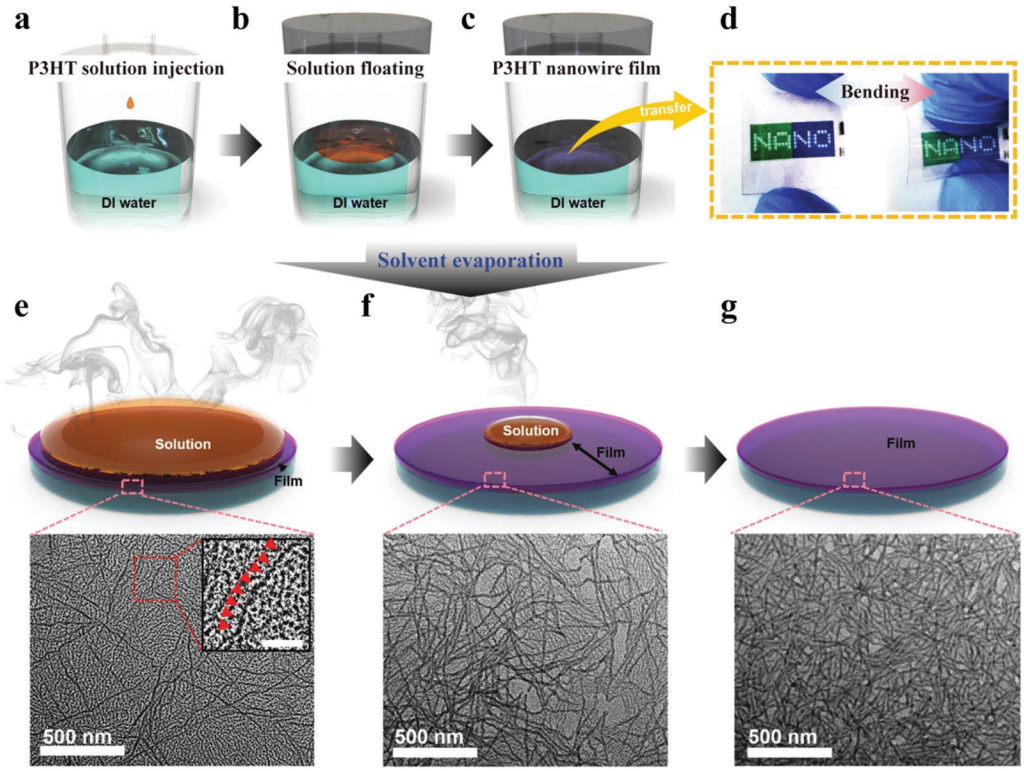

Fig. 7 (a–c) Fabrication of a thin film composed of P3HT NWs. (d) Transfer of the P3HT NWs thin film onto a flexible and transparent substrate. (e–g) Formation of the P3HT thin film through solvent evaporation with TEM images at each evaporation stage. Reprinted with permission from ref. 36. Copyright 2017 Wiley-VCH.

well-dissolved P3HT chains self-assembled into 1D P3HT nanowires with the formation of the thin film simultaneously, as shown in Fig. 7a–c, and the preparation of a P3HT thin film through solvent evaporation and the TEM images were present in Fig. 7e–g.

The method of self-assembly can be served as the simple patterning and alignment of conjugated polymer chains, and this method is suitable for large-scale, low-cost organic electronic devices. Dimensional and morphological features of the resulting patterns or structures can be controlled by the evaporation process including the evaporative flux, solution concentration, interfacial interaction between the solute and the substrate, solute size, and shape, solvent evaporation rate, *etc.* For example, Byun *et al.* demonstrated a versatile and controllable strategy to form hierarchical assemblies comprising concentric rings with a crystallized nanofibrils by confining a single drop of regio-regular (rr) P3HT toluene solution in an axially symmetric sphere-on-flat geometry for evaporation.[37] The simple patterning and alignment of the rr-P3HT chains were successfully controlled by varying the solution concentration. In particular, the rr-P3HT rings with directionally crystallized nanofibrils perpendicular to the electrodes showed enhanced conductivity compared to the rings with randomly distributed nanofibrils. In sharp comparison with other techniques such as top-down lithography, controlled evaporative self-assembly is an uncomplicated and cost-saving strategy to readily produce well-organized structures at the micro-to-nanometer scale.

2.8 Others

In addition to above mentioned methods, some other novel methods have also been developed and applied for synthesizing NCPs. For example, NCPs have successfully been prepared by radiolysis under ambient condition, in which the polymer precursor was polymerized by γ-irradiation, allowing for preparation of pure NCPs without any other additives. Other novel techniques such as pulsed laser ablation in liquid (PLAL) have also been developed to prepare organic nanoparticles (ONPs) and other nanomaterials.[38–41] PLAL has been recognized as a promising technique for preparing organic nanomaterials mainly owing to its simplicity and cost-effectiveness. Under PLAL nanoparticles can be grown by direct laser beam irradiation onto the surface of target material placed in a liquid media. We expect that PLAL will be extensible to the preparation of NCPs upon some appropriate selection of the polymer precursor and modification of the reaction condition.

3. Morphologies of NCPs

The morphological structures of NCPs largely determine their performance so it stands to reason that controlling the morphology can be used to further improve performance. Thus, defining a relationship between morphological structure and performance is indispensable. In this section, we will discuss NCPs with different morphology in detail, including sphere-like,

rod/wire-like, porous-like, and core–shell structure, and offer their physicochemical features and advantages.

3.1 Sphere-like structure

Generally, nanospheres are distinguished with macroscopic objects, owing to their spherical shape, smaller particle size, higher specific surface area, and orderly atoms arranged inside the particle. Sphere-like NCPs have been widely used in various fields such as emerging biotherapy field, which we will discuss in detail below. The sizes, shapes and surface characteristics of nanospheres occupied the key roles in their physicochemical properties. Moreover, nanospheres with diverse morphological structures including porous, urchin-like, and hollow nanospheres have been developed to improve their performance.

Porous CP nanospheres have presented promise in various fields, especially in electrochemical energy storage. For example, Sawant *et al.* synthesized the porous PANI by polymerization of aniline in brine (saturated sodium chloride) solution in the presence of mineral acid dopant.[42] The surface areas of PANI are 57.8 $m^2 g^{-1}$, 68.9 $m^2 g^{-1}$ and 66.8 $m^2 g^{-1}$ by doped with HCl, H_2SO_4 and HNO_3, respectively, which were obviously higher than that of conventional PANI (31.1 $m^2 g^{-1}$). Such porous morphology benefits from a pseudo template, *i.e.* the dissolution of brine solution creates a porous polymer network with voids, leading to a porous and open structure of the PANI nanoparticles. In addition, the porous PANI electrodes showed a high specific capacitance of 662 F g^{-1}, which is 2.5 times greater than that of conventional PANI. Such porous nanospheres not only give larger high surface area and well-defined porosity, but also endow more active units for them.

Similar with porous nanospheres, urchin-like CP nanospheres with high specific surface area endow them good electroactivity, catalytic performance and electro-responsive ability. For example, Hu *et al.* prepared the urchin-like PANI nanospheres with a larger specific surface areas of 267 $m^2 g^{-1}$, and its specific capacitance reached 435 F g^{-1} (10 mV s^{-1}).[43] The ionic diffusion path is related with the various morphology and nanostructure of NCPs when the faradaic reaction occurs at the PANI electrode/electrolyte surface, which has great impact on the capacitances performances. Yang *et al.* synthesized urchin-like polystyrene/PANI composite microspheres by seeded swelling polymerization, and those nanospheres present favourable catalytic performance in the epoxidation reaction of *cis*-cyclooctene with *tert*-butyl hydrogen peroxide as oxygen source.[44] The *cis*-cyclooctene is oxidized in 97% conversion and 92% selectivity using the sea urchin-like microspheres as the catalyst supports. Obviously, the percent conversion have sharply progressed, which originated from the urchin-like surface morphology that endow larger surface area and loading sites, which could increase prominently their catalytic activity and capacity. In addition, Choi *et al.* found that such dedoped urchin-like PANI nanospheres presented dispersed randomly under a 0 V electric field, while arranged in chains when the applied electric field was 300 V, which indicate urchin-like nanospheres have favourable electro-responsive electrorheological ability.[45]

Unlike the above structure, hollow polymer nanospheres have unique porous features due to their hollow nature; properties largely depend on the integrated functionality of the shell materials, the low effective density, and the high specific surface area. These materials have gained tremendous interest due to their numerous desirable properties compared to their solid counterparts. For example, Choi *et al.* reported the hollow PANI nanospheres with higher electrorheological performance than above urchin-like PANI nanospheres, which benefit to form their hollow structure with shorter diffusion length for promoting the electron and stress transfer.[46] Moreover, such hollow structure can be further modified to endow novel performance. For example, Zhang *et al.* prepared mesoporous hollow PPy nanospheres (MHPS) by using chemical polymerization method at the present of silica spheres.[47] These MHPS possess high surface area (117.5 $m^2 g^{-1}$) and pore volume (0.34 $cm^3 g^{-1}$), which provide many sites for supporting Pt nanoparticles. They found Pt/MHPS can be used as a catalyst for methanol oxidation reaction, and the peak current density on the Pt/MHPS catalyst in the forward sweep is 134 mA mg^{-1} Pt, about 1.9 times that of the Pt/XC-72R (73 mA mg^{-1} Pt) catalyst. Dramatically increased surface area, extremely low densities, and a myriad of tailorable functionalities make hollow NCPs a target of numerous research efforts.[47] However, how to precisely control the pore size and maintain long-term stability of porous structure of the cycle of doping and undoping process is remain a challenge. Therefore, in order to fully magnify their performances, proper control over the specific surface area and the corresponding morphology of electrode materials is crucial.

3.2 Rod/wire/fiber-like structures

1D nanostructures stand out for unique combination of their anisotropic optical, mechanical, and electronic properties, thus have developed into a wide range of applications.[48] Compared to nanospheres, 1D NCPs possess higher aspect ratio, which could efficiently transport electrical carriers along one controllable direction.[48] Recent years have seen a lot of emphasis among various researchers to synthesize rod-/wire-/fiber-like NCPs.

CPs with short-rod nanostructures potentially offered the opportunity used in various areas by controlling morphologic structure. In addition, its peripheral contour can be precisely controlled by utilizing the template. For example, Hu *et al.* prepared hexagonal spiral prismatic PPy nanorods by chemical oxidation in the hexagonal spiral prismatic micelles of IC-Fe(II) chelate, and the PPy nanorod has a conductivity of 1.6 S cm^{-1}, which has 3 orders of magnitude bigger than that of PPy film.[49] The lengths and widths of nanorods have a greater impact on their physicochemical properties. For example, Chen *et al.* obtained the PEDOT nanorods with different morphology features by aqueous and reverse-phase micro-emulsion polymerization, respectively, which resulted in great difference for physicochemical properties.[50] The thermoelectric performance of PEDOT nanorods prepared by reverse microemulsion polymerization (8.75 S cm^{-1} for conductivity; 16.2 mV K^{-1} for Seebeck coefficient) was significantly superior than prepared

by aqueous polymerization (0.02 S cm^{-1} for conductivity; 7.11 mV K^{-1} for Seebeck coefficient). As a consequence, the power factor for the nanorods polymerized in the reverse-phase micro-emulsion (0.23 mW m^{-1} K^{-2}) was much higher than that polymerized in water (1.01×10^{-4} mW m^{-1} K^{-2}). It is not difficult to understand that fine nanorods structure is difficult to form favorable π–π stacks and chain-to-chain interactions, which results in poor electrical and thermoelectric properties. In contrast, nanorods with a broad structure can easily create interchain interactions, which is clearly beneficial for improving electrical or thermoelectric performance.

Dependence of the electrical properties on the diameter, which is referred to as the size effect, must be considered for NCPs. Thus, wire (fiber)-like NCPs are developed and most widely used in various electronic devices. In general, a nanowire can be defined as 1D structure with a diameter of less than 100 nm with no limitation in length.[6,12,29] Nanowires have achieved success as building blocks in nanotechnology research and novel concepts in domains traditionally dominated by bulk materials.[12,29] This success mostly relies on the high versatility of these structures both in growth methods and functionality, which opens new grounds for existing and novel applications.[29] Among several interesting properties, nanowires offer two key advantages in the form of their excellent material quality and design freedom associated with their morphology.[29] Because of these unique properties of NCPs, they are of great interest to the broad scientific communities. However, most of NCPs are amorphous or paracrystalline, and possess high density of defects or grain boundaries, which act as trapping sites of charge carriers, thus resulting in decrease in conductivity. CP nanowires have characteristic electronic and optical properties owing to their large length–width ratio; the 1D structure can promote more effective doping and strengthen inter- and intra-chain interactions to enhance the degree of crystallinity, which results in an increase in conductivity. In comparison to amorphous CP, single-crystal CPs exhibit the highest conductivity due to the perfect stacking order of the polymer chains (and thus the 1D stacking order). The high order of crystalline structure also minimizes the formation of defects or grain boundaries, thus with little charge trapping.[51] For example, Sung *et al.* developed single-crystal PEDOT nanowires (Fig. 8a–c) by VPP of EDOT.[51] The single-crystal PEDOT nanowires present an ultrahigh conductivity up to 8.797 S cm^{-1}, which has potentially uses in all organic nanowire interconnects for transparent, flexible, inexpensive, and large-area electronics, such as displays. Such remarkable improvement in the mobility of the single-crystal PEDOT nanowires suggests that their highly crystalline structure with a small π–π stacking distance mainly contributes to the ultrahigh conductivity (Fig. 8d–g). Moreover, such single-crystal PEDOT nanowires can be fabricated into flexible devices on a flexible substrate (Fig. 8h–j).

Thus, the performances of NCPs are closely related to crystallinity and nanoscale of CPs. Recently, some approaches for tailoring crystal morphological structure of NCPs have been performed. For example, Peng *et al.* showed that the P3HT nanofibers can be tailored into nanoribbons associated with the crystallographic transition from edge-on orientation to flat-on orientation by adding the alkylthiols into P3HT nanofibers solution, and the transmission electron microscopy (TEM) and atomic force microscopy (AFM) images of P3HT nanofibers and nanoribbons are shown in Fig. 9a–d.[52] This work demonstrates an efficient strategy to tailor the crystal dimension of P3HT and provides an effective approach to regulate and control the morphology of the polymer.

While the electrical traits of pure CP nanofibers prepared by conventional methods have clear disadvantages such as lower aspect ratio, rough surface, or agglomeration.[5,6,12,29] At present, there are many ways to modify pure NCPs materials, and adding conductive filler is an effective way to enhance their electrical activity. Introduction of nanoparticles into nanowires creates gaps in the segments, which increases the surface area of the nanowires and, therefore, the potential for higher electrical activity than continuous nanowires.[53] Common conductive fillers are mainly metals, metal oxides, or carbon materials.

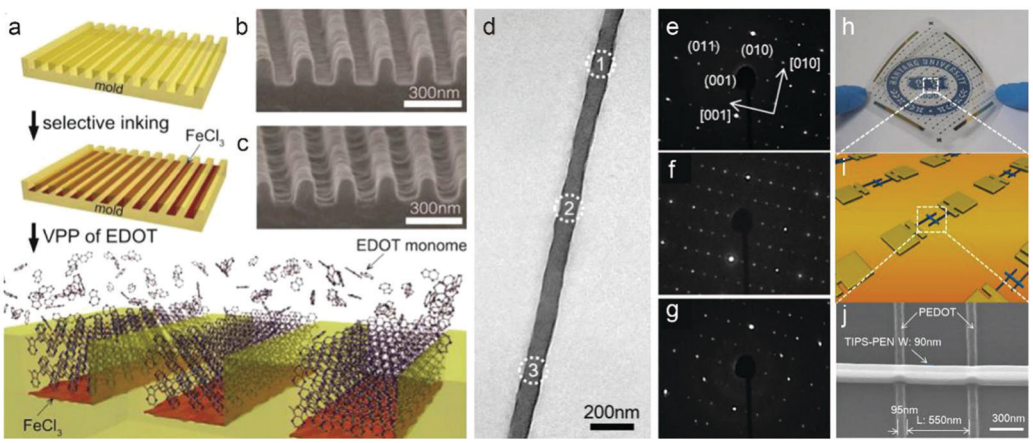

Fig. 8 (a–c) Schematic illustration of the procedure used to fabricate a single-crystal PEDOT nanowire array. (d) The TEM of PEDOT nanowire, (e–g) the corresponding SAED patterns corresponding to three different areas of the PEDOT nanowire. (h–j) The photograph of a nanowire array of FETs and its SEM. Reprinted with permission from ref. 51. Copyright 2014 American Chemical Society.

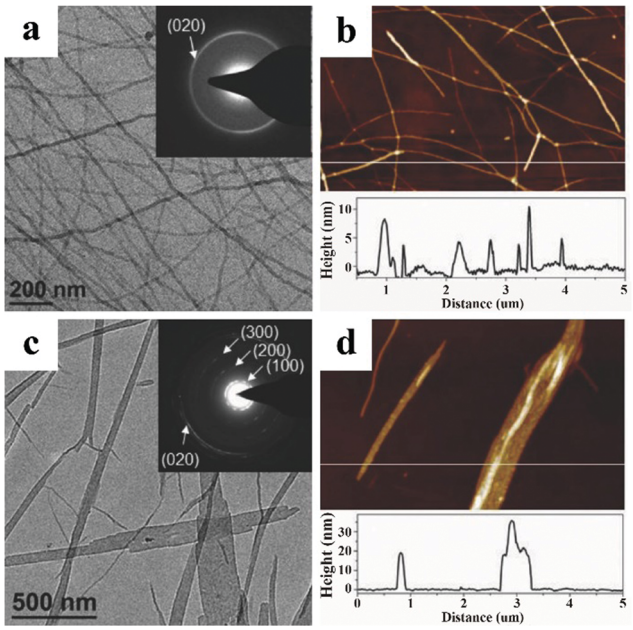

Fig. 9 (a) TEM image of P3HT nanofibers drop-cast from $CH_2Cl_2/CHCl_3$ solution. (b) AFM image along with the line profile of P3HT nanofibers. (c) TEM image of P3HT nanoribbons drop-cast from $CH_2Cl_2/CHCl_3$ solution with the addition of 12-thiol at 30% by volume. (d) AFM image along with the line profile of P3HT nanoribbons. Reprinted with permission from ref. 52. Copyright 2017 Wiley-VCH.

Carbon materials are cheap but complex technological process is not conducive to widespread application. Consequently, metals with good electrical conductivity, especially metal nanoparticles, are widely used to modify the surfaces of CP nanowires. For example, Jang *et al.* found that the Ag nanoparticles attached PPy nanowires (Fig. 10a and b) could increase the photocurrent and spectral response, and the integrated devices have a remarkably high photocurrent density, up to 25.3 times (2530%), under the blue light illumination and wide spectral response.[53] This is due to the intervention of the filler material to some extent to compensate for the surface defects of the material, while good synergy enables the material to produce new properties. Another favorable strategy to improve the performance of NCPs should be construct core–shell structure between NCPs and others active material, we will discuss in below part.

In short, a variety of approaches have been employed to synthesize NCPs with wire-like structures. However, facile, efficient, and large-scale synthesis of the nanostructures of CPs with uniform and non-disperse, and selected morphology and size, and oriented nanostructure arrays, are still challenging. With some strategies, the polymeric structure can offer improved performance in comparison to the bulk case, but fabrication of highly crystalline polymer nanofibers is still difficult.

3.3 Porous structures

Porous structures are given a lot of attention because of their potential to merge the multiple chemical functionalities into the porous framework or the pore surface.[14] Designing a porous structure, down to the micro- and nanoscale range, has long been an important subject, owing to their ability to possess the properties of both porous characteristics and intrinsic polymer materials.[14] Polymers with porous structures can incorporate multiple chemical functionalities into the porous framework or on the surface of the pores. First of all, porous structures have higher surface area per unit volume and well defined porosity.[14] Moreover, the sizes of the pores can be controlled to obtain specific properties.[14] Of course, several important characteristics, including pore geometry, pore size, pore surface functionality, are also being studied in depth for applications involving NCPs. Porous electrode materials have recently drawn a lot of attention because they possess higher specific surface area than bulk materials. Porosity materials with large pore diameter have good electrolyte accessibility, therefore, ionic transport is facilitated, which can lead to a substantial improvement of rate capability.

3.3.1 Nanotubes. Inspired by materials with tube-like structure like carbon nanotubes, CP nanotubes received much attention as one-dimensional structures.[6] Nanotubes with a unique pore structure and high aspect ratio, coupled with the unique properties, have resulted in scientists exploring how best to exploit them.[54] Unlike nanowires, the inside of nanotubes is hollow, which endows them with unique properties in electric and catalytic activity. Template assisted methods are common and effective routes to synthesize CP nanotubes, in which control of the homogeneity, length, and inner/outer diameter of the polymer tubes can be achieved by appropriately choosing of the template, thus making the process inexpensive

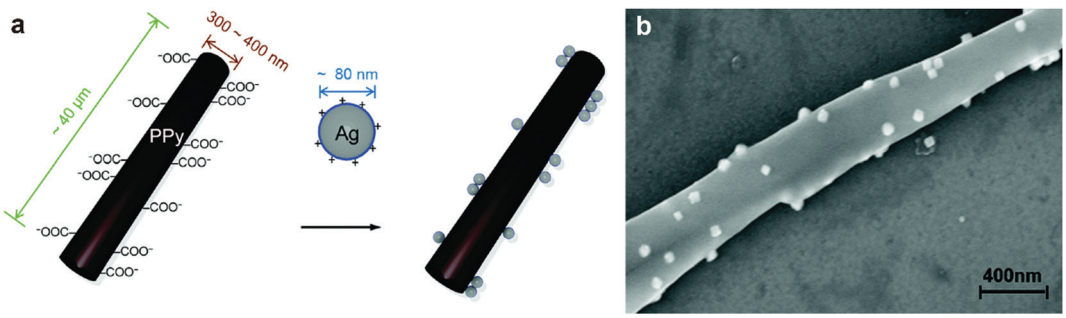

Fig. 10 (a) Schematic diagram of Ag NPs decoration onto PPy NW with electrostatic interaction. (b) A SEM image of PPy AgNPs NW. Reprinted with permission from ref. 53. Copyright 2015 Royal Society of Chemistry.

and simple. For example, Estrany *et al.* prepared hollow PEDOT nanotubes by using electrospun PE44 fibers as sacrificial template, and the length, and inner/outer diameter of the nanotubes can be facile controlled by changing the shapes of template.[55] Notably, the hollow space inside the tubes would provide more surface area for reactions and lead to improved performances. For example, Pang *et al.* prepared PANI with nano-tubular particulate morphology by using urea as soft template.[56] In this process, urea can be aggregated with aniline through H-bonding to form core–shell structured rods, with urea assembly as core and aniline as shell. When the molar ratio of urea to aniline is 3, such PANI nanotubes present superior specific capacitance of 405 F g^{-1} than PANI (263 F g^{-1}) at current density of 0.2 A g^{-1}. Moreover, the maximum energy density for PANI nanotubes sample is 44.97 W h·kg^{-1} (at a power density of 100 W kg^{-1}), which was much higher than the energy density of 29.17 W h kg^{-1} for PANI. The nanotube structures with high specific surface area provide more active sites for electrode reaction. Thus, the prepared PANI nanotubes exhibit high specific capacitance and excellent rate capability.

Similar to other CPs, by combining with other active materials such as silver, gold, or palladium nanoparticles, the performances can be effectively improved for nanotubes with the 1D structure, which made them candidates for antibacterial or catalytic materials. For example, hybrid nanocomposities between PANI nanotubes and carbon nanomaterials, such as single-walled carbon nanotubes (SWCNTs), multi-walled carbon nanotubes (MWCNTs) or graphene (G) and graphene oxide (GO) sheets, have been reported. Recently, Olejnik *et al.* provided a nanocomposities based on PANI nanotubes and multilayered fullerenes, and such nanocomposites exhibit a brush-like architecture with a specific capacitance of 946 F g^{-1} at a scan rate of 1 mV s^{-1}.[57] The higher values of specific capacitance for the nanocomposite result from the high conductivity of both nanostructures, due to their extremely high porosity and organized brush-like structures. In particular, ''conductive'' channels were created in which the interactions between π-electrons of the PANI aromatic/quinonoid structures and multilayered fullerenes facilitate charge transport.

3.3.2 Porous nanofilms. With the rapid development of advanced electronic devices possessing high integration level, the fabrication of ultrathin CPs sheets is becoming increasingly important. Inspired by the unique structure, intriguing electronic and physical properties of graphene, increasing attentions have been devoted to exploring novel 2D nanomaterials.[58] Currently, 2D sheet-like materials are one of the most promising components of device assembly due to their favorable planar layered structure.[59] Tremendous efforts have been devoted to developing of novel 2D materials, because of their intriguing properties, such as large surface areas, high mechanical strength, and amplified electronic and optical properties.[60] Among, the creation of mesopores with sizes of 2–50 nm in 2D nanosheet materials are now emerging as an attractive goal, which renders 2D nanosheets with an interconnected network of pores, well defined arrays of pores, and large specific surface area, thereby leading to enhanced electrochemical and catalytic activity and selected filtration capability.[61] Compared with planar nanosheets, nanoporous nanosheets can increase molecular interactions by providing more active sites for chemical reactions owing to their large specific surface areas.

When a large number of mesopores appear on the surface of ultra-thin nanofilms, their properties will change greatly, especially in terms of electrochemical properties. Although we have discussed in detail the existence of nano-spheres with porous structures above, they are not identical. The appearance of mesoporous on the surface of nano-thin films may affect their conductivity to some extent, but at the same time, it will also bring new properties, such as higher electrochemical activity, electrocatalytic ability and so on. The surface of NCPs nanosheets can also be prepared into mesoporous-like by utilizing template, electrodeposition, chemical bath deposition method, *etc.* But the pore sizes are easier to control by prepared templates, thus the nanofilms could present uniform porous structure. For example, Feng *et al.* synthesized 2D mesoporous PPy nanosheets with controlled pore sizes by using block copolymers as dual-template.[61] The two-layer template gives the polymer film a characteristic topography on both sides, which gives the polymer film a uniform chemical property. The porous nature endows a higher specific surface area that provides more electrochemically active sites and electrolyte-electrode interfaces for ion storage, thus improving their specific capacity. Upon template removal by extraction with solvents, 2D mPPy nanosheets are achieved with controlled pore sizes in the range of 6.8–13.6 nm, ultrathin thicknesses of 25–30 nm and high surface areas up to 96 m^2 g^{-1}. Serving as cathode materials for Na-ion batteries, the 2D mPPy nanosheets with such a unique structure exhibit a high ion storage capacity of 123 mA h g^{-1} at 50 mA g^{-1}, satisfactory rate capability and excellent cyclability.

3.3.3 Three-dimensional macroporous structure. Inspired by the vertically-aligned 2D nanosheets, CPs were developed into such structures and arranged to form three-dimensional superstructures. They are quite different with the above mentioned porous nanofilms materials in the form of arrangement, which is a little similar to the interactive nanowalls. For example, Mai *et al.* synthesized the vertically aligned PPy nanosheets on three-dimensional (3D) Ni foams *via* a facile template-free method in an environmentally friendly solvent; this process is shown in Fig. 11a.[62] Such sheets possessed an average thickness of 14 ± 2 nm (Fig. 11b) and an average height of 294 ± 34 nm. The schematic representation of the assembly of the PPy–Ni//AC–Ni flexible all-solid-state asymmetric supercapacitor is presented in Fig. 11c, and exhibited a high specific capacitance of up to 38 F g^{-1} at 0.2 A g^{-1} (Fig. 11d). Such structures break the limitation of the original planar structure and realize the longitudinal growth of the polymer, which provides theoretical support for the development of the new NCPs structure. They appear large on the macroscopic scale, but the interior has a delicate 3D nanostructure, which brings a high level performance in electrochemical performance, bringing great potential for the development of innovative electronic materials.

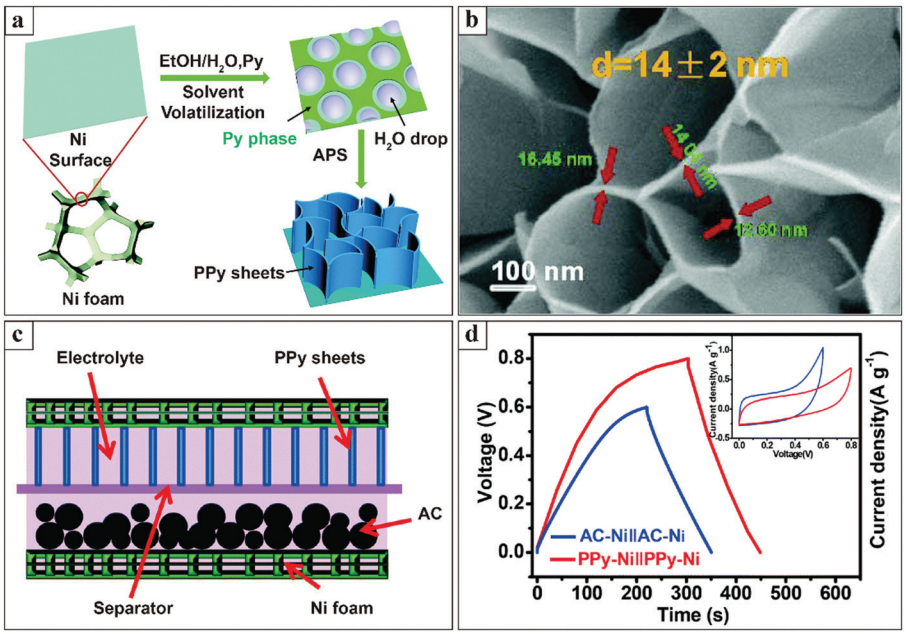

Fig. 11 (a) Schematic illustration of the facile template-free synthesis of vertically aligned PPy nanosheets on Ni foams. (b) SEM images of the nanosheets (c) Schematic representation of the assembly of the PPy–Ni//AC–Ni flexible all-solid-state asymmetric supercapacitor with the PVA/$LiClO_4$ electrolyte. (d) Charge/discharge and CV curves of the symmetric supercapacitors. Reprinted with permission from ref. 62. Copyright 2016 Royal Society of Chemistry.

Recently, CP hydrogels with 3D nanostructure provided intrinsic molecular frameworks that promote the transport of charges, ions. Owing to their polymeric nature and synthetic tunability, CP hydrogels combine the advantageous features of conventional gel materials and inorganic conductors, thus showing superior properties.[1,4] The unique 3D porous nanostructure constructed by the interconnected polymer networks endows CPs hydrogels with good mechanical properties and high performance acting as electrode materials.[1,4] For example, the conductivity of pure CP hydrogels is from 10^0 to 10^3 S m^{-1}, and the Young's modulus is from 10^0 to 10^3 kPa.[1,4,63] Although CP hydrogels possess above numerous advantages, their performance are also affected in many crucial factors. Firstly, the conductivity and electrochemical properties of CP hydrogels can be tuned over a wide range by changing the crosslinkers, which also act as dopants.[1] The conductivity of the polymer depends highly on the used dopants and the level of doping. This tunable conductivity enables CP hydrogels with the ability to serve as insulators, semiconductors, or conductors for a range of applications.[1] Moreover, the mechanical properties of CP hydrogels can be improved by controlling their nanostructures.[64–66] Traditional CPs show poor elasticity owing to their rigid backbones brought about by a highly conjugated structure. By forming an interconnected hollow sphere geometry, CP hydrogels can exhibit an effective elastic modulus capable of withstanding large effective strains and stresses.[1,64,66] For example, a PPy gel foam with a hollow sphere structure displays a high modulus and reversibility in cycles of compression tests, demonstrating good mechanical elasticity.[64] Moreover, the unique 3D porous nanostructure constructed by interconnected polymer nanospheres endows PPy hydrogels with high performance acting as supercapacitor electrodes with a specific capacitance of 380 F g^{-1}, excellent rate capability, and areal capacitance as high as 6.4 F cm^{-2} at a mass loading of 20 mg cm^{-2}. Such PPy hydrogel in the dry state showed the conductivity of 0.5 S cm^{-1}.[64] Their porous structure not only provides larger high surface area and well-defined porosity, but endow increases the contact with active units for CP nanoparticles that present higher electroactivity than non-porous materials. Thus, they are advantageous in electrochemical energy storage, but precisely control of the pore size and maintaining the long-term cycling stability in charge and discharge process remain challenging.

3.4 Core–shell structures

Novel and improved performances can be achieved by assembling with other active materials to construct core–shell structure nanocomposites. The unique coating has the potential to decrease the surface energy, which reduces the potential for aggregation as well as limiting the side reactions between electrolyte and electrode, resulting in improved reversibility and cycling stability of the electrodes.[67] The construction of composite electrode materials can combine the advantages of each component.[12] Core–shell nanocomposites are highly electroactive materials with modified properties that arise from either the core or shell materials. Furthermore, the properties can be modified by changing either constituents or the proportion of the core to the shell. The properties of the core particle such as electrochemical activity or stability can be modified by the shell material, increasing the overall particle stability and capacitance.[68]

Generally, CPs (including NCPs) must be doped (often by oxidation or adding dopants) to maintain their signature

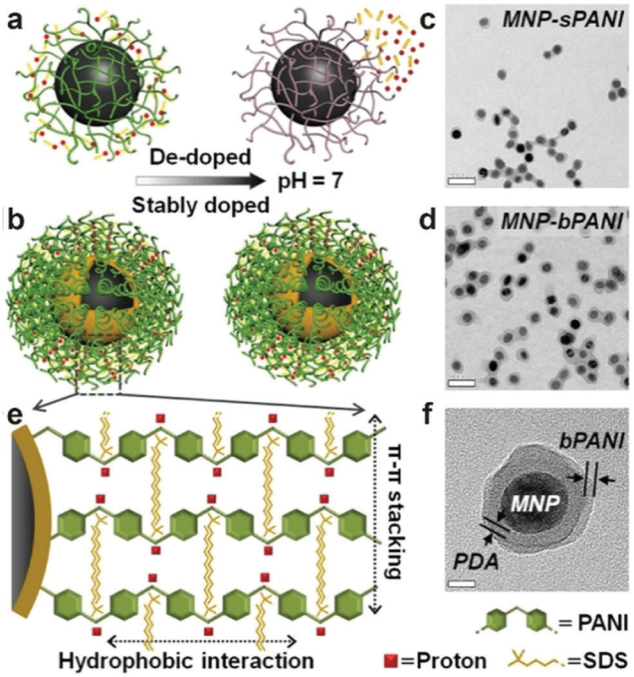

Fig. 12 (a) Scheme illustrating conventional loosely packed PANI (spaghetti-like). (b) Densely packed brush PANI with excellent doping stability. (c and d) TEM showing successful coating of PANI nanoshells on MNPs. Scale bar, 100 nm. (e) Diagram illustrating high-density PANI brush polymerized on an intermediate PDA layer. (f) TEM showing PDA–PANI dual shell layers on a MNP. Scale bar, 20 nm. Reprinted with permission from ref. 69. Copyright 2018 American Chemical Society.

electrical and optical properties, but these dopants are not permanently "integrated" into the polymer backbone and are, thus, susceptible to dissociation.[69] Once the doped ions are removed from the polymer chain, the CPs lose electrical conductivity, which has largely limited their application. Therefore, guaranteeing long-term stability of dopants in polymer chains is vital for their practical applications. Gao *et al.* prepared a densely packed PANI brush on the surface of magnetic nanoparticles (MNP) by surface initiated polymerization and the design schematic is presented in Fig. 12a and b.[69] TEM images showed successful coating of PANI nanoshells on MNPs (Fig. 12c and d). Such brush-like MNP-PANI (Fig. 12b) nanocomposites could maintain the doped states (*e.g.*, color) after repeating rinsing with phosphate buffer solution (PBS), and distinct near infrared extinction at physiological pH. The increase in environmental stability was ascribed to the core–shell structure with the bushy polymer network (Fig. 12e and f). Similarly, the problem of aggregation between nanoparticles can be effectively solved by constructing such core–shell structure. For example, coating a water-soluble macromolecule, *e.g.* poly(vinylpyrrolidone) (PVP), could suppress undesirable interactions between PANI nanoparticles and significantly enhance the dispersibility of NCPs, which originated from the pyrrolidone group in PVP can strongly interact with PANI chains by hydrogen bond.[69]

NCPs with 1D structure can also be synthesized as core–shell structures by compounding with inorganic materials, metals, or metal oxides, and can be implemented as the core or as the shell part.[70,71] Generally, 1D nanomaterials with core–shell structure combine the intrinsic properties of each component to obtain, for example, higher electrical conductivity, greater electrochemical reversibility, shorter ionic transport, and improved mechanical stability, and cycling stability.[70,71] For example, Li *et al.* prepared α-Fe_2O_3@PANI core–shell nanowire arrays by depositing PANI on the surface of α-Fe_2O_3 nanowire arrays (Fig. 13a).[72] PANI covering the surface of Fe_2O_3 nanowires is observable in Fig. 13b–e, with the diameter of Fe_2O_3 nanowire of ~20.3 nm and the thickness of PANI shell is ~8.3 nm. Compared with pure α-Fe_2O_3 electrode, the α-Fe_2O_3@PANI electrode has better electrochemical performance with a tripling of C_{sp} from 33.9 to 103 mF cm^{-2} and superior cycling stability.[72] The design of electrode materials with a nanowire array structure is attractive for achieving high performance in terms of electrochemical energy storage due to their large surface area, short diffusion paths for ions and electrons, and structural stability during cycling. As a result, such arrays-like structures not only increase the specific surface area of the material, but also shorten the ion transport path due to the vertical structure, which allows ions to travel at a higher rate in the nanowire matrix. The nanowire matrix structure has several advantages, for example: (1) each nanowire is electrically connected to a conductive substrate; (2) the nanowire matrix has an one-dimensional vertical electronic path which is a guarantee for efficient charge transfer, and reduces the length of ion transport to increase efficiency; and (3) the gap between the aligned nanowire matrix columns can accommodate a large amount of micron sized material.[73,74]

Satisfactory performance is based on a reasonable structural design. The core–shell structure is a promising design approach because it accommodates the synergistic advantages of two materials. The internal structure can be customized according to performance requirements, which makes it possible to develop new material systems with excellent performance. The performance of functional materials is governed by their ability to interact with surrounding environments in a well-defined and controlled manner. Coating technologies provide an opportunity to control the surface of a material, thus creating composite materials where the interface and the bulk of the material can, to a large extent, be engineered and controlled independently. However, precisely controlling the coating layer thickness and appropriately matching the core and shell are remaining research topics.

4. Applications

Over the past decade, NCPs and their composites extensively served as building blocks to construct new cutting-edge electronic and biological materials/devices. The diversified structures of NCPs endow them a wide range of applications because they can be customized to possess target properties. In this section, we systematically summarize the major applications of NCPs, such as biological therapeutics, biosensors, microwave absorbers for electromagnetic shielding, and various energy storage/conversion/saving devices.

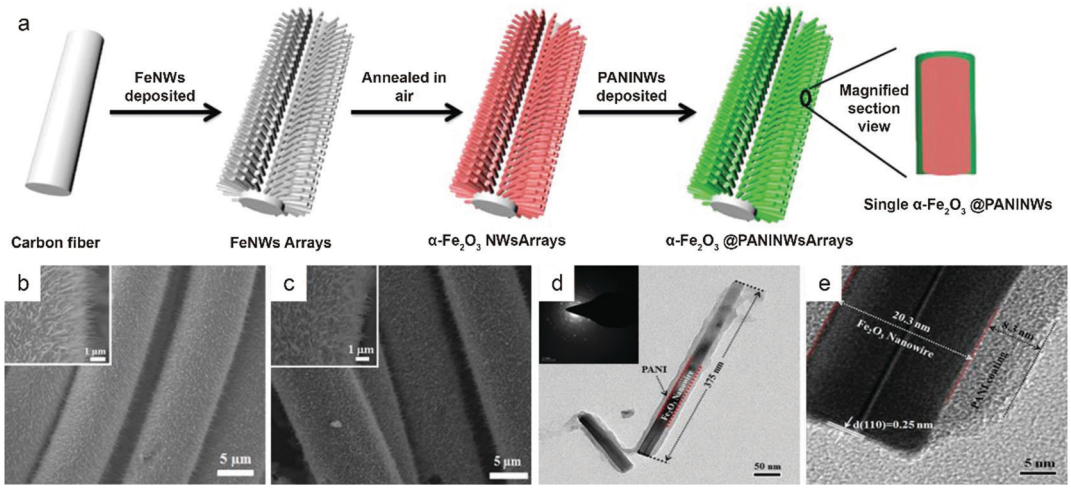

Fig. 13 (a) Schematic illustration of the electrode fabrication and a magnified view of a single α-Fe_2O_3@PANI core–shell nanowire structure. EM images of (b) α-Fe_2O_3 and (c) α-Fe_2O_3@PANI; (d) TEM image, (e) HRTEM image, and (c, inset) the corresponding SAED pattern of the α-Fe_2O_3@PANI core–shell nanowire. Reprinted with permission from ref. 72. Copyright 2015 American Chemical Society.

4.1 Biological therapeutic

Advances in nanoscience engineering, as well as developments in understanding the importance of nano-materials characteristics such as size, shape, and surface properties for biological interactions, are creating new opportunities for revolutionizing the diagnosis and treatment of many diseases such as cancer, pain and infectious diseases.[75] Scientists have demonstrated that NCPs have potential use in biomedical applications including drug release and accumulation, neural prostheses, photothermal therapy and imaging, *etc.*[76,77] Compared to many existing inorganic nanoparticles, as well as small organic dyes currently explored in biomedicine, NCPs show exceptional optical and chemical stability, lower toxicity, and better biocompatibility, making them highly attractive for biological applications.[78] In addition, their unique π-conjugated structures could lead to their excellent photostability and high photothermal conversion efficiency in the near-infrared region.[77]

As far as photothermal therapy is concerned, CP nanoparticles are promising as photothermal coupling agents due to their high photothermal transformation efficiency, robust photostability, good biocompatibility, and low expense.[79] Upon photoexcitation, NCPs complexed with photosensitizing molecules can sensitize the oxygen molecule to readily produce reactive oxygen species (ROS) including singlet oxygen by either direct sensitization of CP composites or indirect sensitization *via* energy transfer.[80] ROSs are widely recognized for effective killing of bacteria or cancer cells in proximity.[80] Unfortunately, many unmodified CPs are hydrophobic, while hydrophilicity is required for biological therapeutics. With the above-mentioned advantages features, the modification of the surface of NCPs by employing benign water soluble (biocompatibility) materials is promising. For example, Liu *et al.* fabricated PPy nanoparticles by using bovine serum albumin (BSA) as the stabilizing agent, and PPy@BSA-Ce6 nanoparticles exhibited good biocompatibility, little dark toxicity to cells, and were able to trigger both photodynamic therapy and photothermal therapy.[78] Similarly, coating PVP on the surface of PANI resulted in biocompatibility and such nanocomposites combined with NIR irradiation presented excellent photothermal conversion performance, which could kill cancer cells *in vitro*.[62]

Recent developments indicated that NCPs can be used as neural and osteogenic implants for signal recording and electrical stimulation due to their electroactivity and biocompatibility. Notably, in the field of neuroscience, it is still a major challenge to regenerate a damaged nervous system. Cai *et al.* found that cells cultured on the nanoporous cellulose gels (NCG)/PPy composite extended multiple long neurites with or without a dopant (Fig. 14a and b).[81] Therefore, NCPs hold promise in transducing nerve stimulation at the cellular level, and thus can be applied to a neural electrode interface for neural repair and regrowth (Fig. 14c–e). Under electrical stimulation the nerve

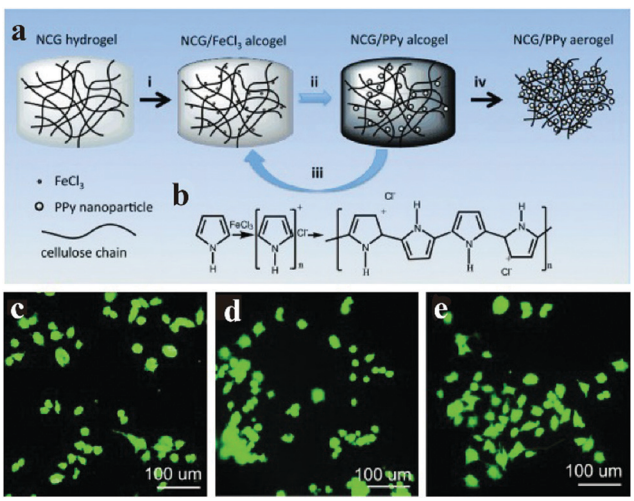

Fig. 14 (a and b) Preparation of NCG/PPy composite aerogels. (c–e) Fluorescence micrographs of PC12 cells cultured on different composite gels after electrical stimulation. Reprinted with permission from ref. 81. Copyright 2014 Wiley-VCH.

conduits that possess a similar conductive function as myelin sheath of the nerve can stimulate the outgrowth of nerve and axon regeneration, and finally achieve the repair of nerve injuries.

Similarly, Zhang *et al.* synthesized the PANI/cellulose composite hydrogels with good mechanical properties (tensile strength from 1.08 to 2.71 MPa) and biocompatibility, which showed excellent guiding capacity for the regeneration of sciatic nerves in adult Sprague-Dawley rats without any extra treatment.[82] On the basis that the pure cellulose hydrogel was an inert material for the neural repair, PANI played an indispensable role on the peripheral nerve regeneration. The hierarchical micro–nano-structure and electrical conductivity of PANI remarkably induced adhesion and guided the extension of neurons.[82]

Such discoveries have opened new frontiers of biomedical healing and evoke hope for overcoming challenges that have plagued medicine for years. However, these implants in organisms often fail due to bacterial infection, which seriously limits applications as biological therapeutics.[83] Therefore, improving antibacterial properties is essential for further developing biological therapeutic materials. Ning *et al.* reported the PPy nanocomposites with antibacterial properties by employing the biomolecule sulfosalicylly acid (SSA) *via* template-free electrochemical polymerization.[83]

In addition, NCPs show great promise as drug release technology (*e.g.*, chlorpromazine, insulin). A stimulus to control the release of therapeutic drugs based on electrical potential could be advantageous because it can tuned to release only under specific conditions (the current/potential magnitude and frequency) with precise, local, continuous, and reversible features.[84] Electrochemically controlled drug release based on NCPs is among the most interesting drug delivery systems, as NCPs with incorporated drugs can be easily synthesized on conductive substrates to form different shapes and patterns, and the release can be precisely controlled by applying electrical current or potential stimuli for reversible polymer redox reactions.[84] However, precisely controlled drug release from the thin films under mild conditions is still a challenge.

Combining NCPs with other biocompatible materials to construct biotherapy materials is a promising method to create advanced biological therapeutics. This platform technology is expected to open exciting opportunities to overcome intractable diseases. It reveals new opportunities for synthesis and design of inspired medical conductive biomaterials, but the fabrication of unique nanostructures still remains challenging.

4.2 Biosensors

Biosensors gained attention due to the ability of NCPs to emulate biological systems to a certain extent and take non-invasive measurements of various functional indicators of the human body.[85] In general, biosensors could take a real-time, onsite, simultaneous detection of determinants. However, the complex and changeable environments within organisms bring serious difficulty in detection, especially in human baby, which requires the sensor to have high sensitivity and selectivity.[86] As described in above, NCPs change from an initial insulating state to an electrically conducting state after chemical or electrochemical doping with oxidizing or reducing agents.[12] This transition can be used in such applications as biosensors and their advantageous are summarized as follows: (1) the properties of NCPs can be tailored to detect a wide range of chemical compounds because the conductivity is sensitive to dopant type and degree; (2) the sensitivity of NCPs-based sensors is enhanced compared to the bulk material-based sensors due to the high surface-area of the NCPs; (3) response time of the nanostructure-based sensors is shorter than non-nanostructured sensors because the porosity of the nanostructures enables gas molecules to diffuse in and out of the nanostructures rapidly.[12,87–90]

In recent years, a variety of CP nanocomposites with graphene and noble metal materials, *etc.* are used them in electrochemical methods to detect biological characteristic reagents, such as prostate specific antigen, carcinoembryonic antigen, *etc.*[91–94] For example, Zhang *et al.* prepared core–shell structure nanofibers based on PEDOT and multi-walled carbon nanotubes, such nanocomposites presented good detection capability for magnolol, and less than 0.003 μM magnolol could be detected.[93] Gao *et al.* proposed a novel electrochemical sensor based on porous overoxidized polypyrrole/graphene nanocomposites, and this sensor can detect adenine and guanine with a linear range covering 0.06–100 mM and 0.04–100 mM, and a low detection limit of 0.02 μM and 0.01 μM, respectively.[94]

Recently, a class of gas sensors with independent detection capabilities was developed into electronic nose systems, aiming to improve the selectivity and sensitivity of biosensors. It has potential use in breath measurements, which could diagnose certain diseases beforehand (*e.g.*, lung cancer) by detecting volatile organic compound (VOC) biomarkers in exhaled breath.[95] This attractive research with huge social impact motivated many researchers to develop novel sensing materials suitable for this application, *i.e.*, the detection of extremely low gas concentrations and VOCs in exhaled human breath.[95] Breath analysis is non-invasive and simple. Previous breath-analysis tools were inconvenient because of a lack of portability, expensiveness of the equipment, and complexity of their operation.[12,90] Therefore, highly efficient, simple, inexpensive, and real-time breath sensors are essential for early diagnosis of disease by breath analysis.[12,90] Nanomaterials are considered as efficient sensing materials with superb sensing capability, owing to their unique nanoscale features and high surface-to-volume ratio.[12,91,94,95] These sensors rely on changes in the electrical resistance of the sensing materials arising from their interaction with VOC biomarkers. Kim *et al.* fabricated biosensors by coating PEDOT on the surface of Fe_3O_4 magnetic nanoparticles (MNPs).[95] These sensors exhibited a significantly higher sensing response to 1 ppm acetone vapor analyte, *i.e.*, a 38.8% higher sensitivity and an 11% lower noise level, which is present in the exhaled breath of potential lung cancer patients, and low noise level.[95]

Nowadays, electronic devices have a tendency to get smaller and more highly integrated due to the development of micro and nano fabrication techniques. With the device thickness down to the micron scale, flexible design becomes an alternative

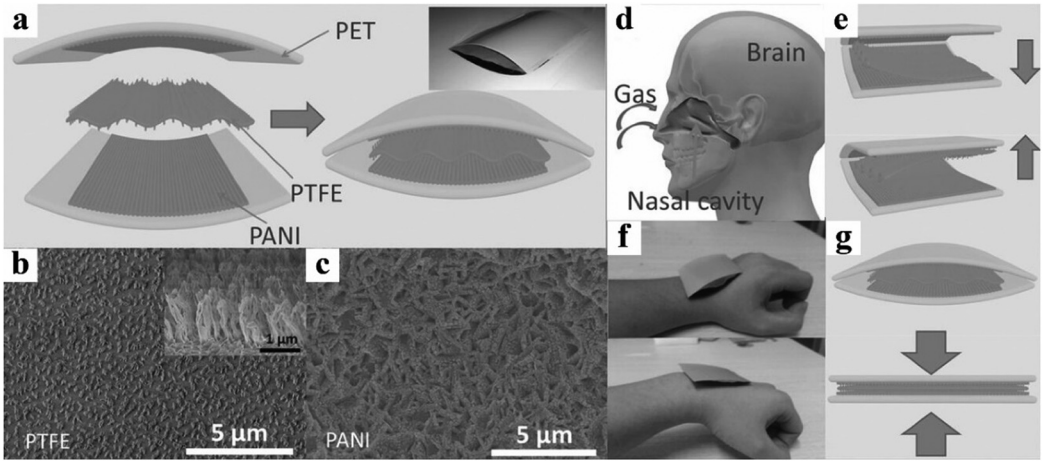

Fig. 15 (a) Structure and fabrication process of the flexible smelling e-skin. The inset is the photograph of the e-skin. (b) SEM image of PTFE nanostructures on the top view. The inset is cross-section SEM image of PTFE nanowires. (c) SEM image of PANI nanostructures on the top view. (d and e) The e-skin can be easily driven by gas flow (human breath or blowing). (f and g) The e-skin can be easily driven by body motion (pressure). Reprinted with permission from ref. 97. Copyright 2016 Wiley-VCH.

for devices to maintain basic mechanical stability as well as offering versatility in designs and large area compatibility.[12,91,94,96] Yun *et al.* reported a flexible field-effect-transistor (FET) biosensor based on 2D PANI nanostructures.[96] With the 2D PANI nanostructure being as thin as 80 nm and its extremely large surface-area-to-volume (SA/V) ratio, the developed flexible biosensor exhibited outstanding sensing performance in detecting B-type natriuretic peptide (BNP) biomarkers, and was able to achieve high specificity (on average 112× over interferents) with the limit of detection as low as 100 pg mL^{-1}.[96]

A more important feature of NCPs is that they can coexist with other electronic devices for biosensors, such as electronic skin. Many researchers have developed e-skins that can sense pressure, tactile, and temperature.[97] Zhang *et al.* reported a flexible electronic skin by building a sandwich-like nanostructures based nanostructured PANI and polytetrafluoroethylene (Fig. 15a–c).[97] The electronic skin can be driven by human motion/breath and efficiently convert mechanical vibration into electric impulse additionally (Fig. 15d–g). The detection limit of the e-skin at room temperature is 30 ppm, and the response is up to 66.8 upon exposure to 210 ppm ethanol.

The above studies show the importance of nanomaterials for biosensor development. The high surface area, porosity, and unique properties of nanomaterials facilitate a low limit of biomolecule detection. The development of nanostructured biosensors is critical for further advancing the field of medical diagnostics.[12] Meanwhile, the miniaturization of integrated sensors and the challenge of supplying power are present challenges. Currently, most of the emphasis in biosensors for human use has been on wearable monitors for glucose. Glucose level is a critically important biomarker for diabetes and its direct measurement in blood requires painful blood sampling that can lead to scarring of the pinprick sites.[98] As an alternative, non-invasive wearable sensors that monitor glucose concentrations in interstitial fluid using needles have been actively studied and commercialized in recent years.

4.3 Microwave absorbers

Electromagnetic interference (EMI) is receiving increased emphasis due to the extensive utilization of communication devices, *e.g.*, telecommunications, local area network systems, and radar systems, which not only cause damage to electronic equipment, but also negatively affect human health.[99] However, the conventional shielding materials are actually unable to dissipate EM emission entirely due to their reflective nature to incident EM waves, and worse than that, they also produce secondary/repeated EMI pollution.[100] Carbon nanotube (CNT) reinforced polymer composites are a typical example, which are the most extensively studied materials for radar absorbing applications.[101] CNTs-based lightweight broadband structures or materials are difficult to fabricate. Therefore, developing novel microwave absorbers is an active research area.

Recently, CPs with π-conjugated main chains demonstrated potential as microwave absorbing materials due to their delocalized electronic structure which endows them with electrical conductivity, low energy optical transitions, low ionization potential, and high electron affinity.[99,100,102] Early, CPs were widely studied as EM shielding materials. It was found that the shielding process of CPs includes both reflection and microwave absorption behavior.[103] To date, CP-based microwave absorbing materials have made significant achievements in this field through rational design of microstructures and hybridization with different types of materials.[104] Although significant progress has been made in these conventional CP-based composites, a gap to real industrial applications still exists because current composites cannot fulfill the particular demands for microwave absorption. Consequently, strict customization of the material structure is necessary, which requires constructing a nano-sized platform for CPs. The frequency range of absorption is still less than the expected bandwidth, so that increasing the thickness of the absorber or using a multi-layer configuration is adopted to broaden the response frequency range in most research cases.[99,100]

For example, Xu *et al.* reported a novel "egg-like" composite of Fe_3O_4 microspheres and PANI by a two-step oxidative polymerization, and they found that embedded Fe_3O_4 microspheres would not only modulate the relative complex permittivity but also had improved reflection loss of −31.3 dB at 9 GHz with a thickness of 3.0 mm.[99]

Research using NCPs has shown potential for microwave absorbance, but further development is required for commercial application. Rational design idea to modify NCPs-based microwave absorbing materials could present high microwave absorbance to mitigate the effects of electromagnetic radiation.

4.4 Energy storage/conversion/saving devices

Novel energy conversion, storage and saving methods are being urgently pursued by scientists to reduce the consumption of increasingly depleted fossil energy. To solve this problem, making increasing the efficiency of energy use and developing clean, renewable energy sources are necessary. Amidst the race to develop materials that may resolve such issues, the advancement of thermoelectric devices (TEs) and supercapacitors (SCs) as well as electrochromic devices (ECs) stands out as promising new technologies to reinforce traditional energy conversion/storage/saving devices.[105–115] NCPs possess high electrical conductivity, large surface area, short path lengths for charge and ion transport, and superior electrochemical activity which make them suitable for above applications. In this section, we summarize the recent advances of NCPs in energy conversion and storage devices, including TE, SC and EC applications.

4.4.1 Thermoelectric. Thermoelectric materials are crucial in renewable energy conversion technologies because they convert waste heat into electricity directly, potentially improving the efficiency of energy conversion.[116–119] The key evaluation factor of thermoelectric performance is so-called dimensionless thermoelectric figure-of-merit (ZT), which is defined as ($ZT = S^2\sigma T/\kappa$).[116] where S is the Seebeck coefficient, σ is the electrical conductivity, T is the absolute temperature, and κ is the thermal conductivity. In principle, the value of ZT results from material properties and the three parameters, S, σ and κ, are interdependent.[117] Currently, inorganic nanomaterials have reached ZT values around 2.6 at operating temperature, which exceeds thermoelectric materials based on CPs (ZT values of 0.42).[120,121] As for CP-based thermoelectric materials, they usually present low intrinsic thermal conductivity form 0.1 to 0.5 W m^{-1} K^{-1}, thus their thermoelectric performance has always been defined by the power factor ($S^2\sigma$) instead of ZT. In comparison to inorganic thermoelectric materials, the random orientation of the molecular chains in amorphous regions seriously reduces the conductance of CPs, which may the main reason for the low power factor value.[116,118] Nevertheless, organic conjugated materials also have advantages in low cost, flexibility, processability, low intrinsic thermal conductivity, and ease of structural modification.[119] In the past 20 years, thermoelectric materials based on CPs have increased in performance by improvements to preparation strategies. Our group demonstrated a PEDOT-based thermoelectric device in 2008, while the ZT value is only 1.75×10^{-3}.[122] Afterwards, the representative achievement of PEDOT aspects were summarized and reviewed.[96] The improvement in power factor of CPs has been considered to be a vital method to increase their thermoelectric conversion efficiency because CPs have inherently low thermal conductivities near room temperature.[121]

The involvement of nanotechnology has brought opportunities for development in the field of thermoelectrics, especially for NCPs. Indeed, the thermo-electric figures of merit of nanostructured materials have been greatly enhanced compared to those of the bulk counterparts in the last decade. In particular, by manufacturing low-dimensional or nanostructured materials such as nanorods, nanowires and nanotubes have been considered as one of the effective strategy to improve the thermoelectric performance of NCPs (Table 1). Compared to their bulk counterparts, considerable enhancements in both electrical conductivity and Seebeck coefficient have been achieved with these nanoscaled conducting polymers due to the highly orientated order of the polymer chains and enhanced carrier mobility within the 1D nanostructrues.

Overall, NCPs for thermoelectric applications are very promising due to enhanced power factors. In addition, the film- and fiber-based or other nanomaterials displayed these advantages for flexible or wearable thermoelectrics energy conversion devices. Employing nanoscale CPs into thermoelectrics devices may be

Table 1 Summary of the thermoelectric properties of 1D nanostructured conducting polymers

Polymer morphologies	Preparation method	σ / S cm^{-1}	PF_{max} / μW m^{-1} K^{-2}	κ / W m^{-1} K^{-1}	ZT	Ref.
PEDOT nanowires	Hard template	43 ± 5	3.4	—	—	123
PEDOT nanowires	Hard template	12	8.7	—	—	124
PEDOT nanofibers	Reverse microemulsion	71.4	16.4	—	—	125
PEDOT nanowires	Hard template + post-treatment	541	23.4	—	—	126
PEDOT nanorods	Aqueous phase	0.02	1.01×10^{-4}	—	—	50
PEDOT nanorods	Reverse microemulsion + post-treatment	16.9	0.91	—	—	50
P3HT nanofibers	Whisker method and silver doping	18.3	6.84	0.80	2.6×10^{-3}	127
P3HT nanofibers	Whisker method	12.6	3.7	0.0708	1.6×10^{-2}	128
PPy nanotubes	Soft template	9.81	0.31	0.17	5.71×10^{-4}	129
PPy nanowires	Soft template	22.5	0.3	—	—	130
PPy nanowires	Soft template	2.217	0.023	—	—	131
PANI nanowires	Soft template and soft template	0.0077	0.035	0.21	4.86×10^{-5}	132
PANI nanowires	Soft template and soft template	1.24	0.028	0.32	2.75×10^{-5}	133

critical strategies in resolving the hotspot cooling issues in microelectronics.

4.4.2 Supercapacitors. Among various electrochemical energy storage systems, supercapacitors (SCs) have been widely investigated in both academia and industry due to their high power density, long cycling life, safety, and low maintenance costs.[134] CPs have been regarded as promising pseudo-capacitive materials because of their unique characteristics and they are expected to improve the energy storage devices as a result of the redox reaction used to store charge in the bulk of the material.[135] Recent studies showed that nanostructured CPs can offer increased power density and specific capacitance.[136]

Since the capacitance in redox supercapacitors is mainly produced by the fast faradaic reaction occurring near a solid electrode surface at an appropriate potential, a relatively short diffusion path can be provided by nanostructured materials to improve the power density of supercapacitors.[137,138] Therefore, electrode materials composed of NCPs have recently received consideration for supercapacitors. In addition, porous nanostructures increase the contact area between electrolyte and active materials. These two features lead to fast reaction kinetics. Electrode materials in supercapacitors essentially involve processes at the interface between an electrode and an electrolyte solution.[139] Increasing the area of the interface is expected to increase the rate of the process. Porous electrode materials with high surface area per unit volume, especially with structural elements on the nanometer scale, have received considerable attention. Thus, active electrodes with meso- or nanoporous structures and good conductivity are highly desirable for high power densities.[140]

While pure CP electrodes (including NCPs) present challenges, especially low energy density, low power density, and poor cycling stability in long term charge–discharge processes. To solve these troublesome problems, several strategies have been developed. Firstly, synthesis of NCPs with designed morphology and/or structure (*e.g.* nanotube). The capacitive performance was improved by increasing crystallinity, controlling microstructure, and controlling surface morphology by adjusting the polymerization method, dopant content, oxidation level, type of surfactant, surfactant content, and so on. Second, synthesis of various NCP composites with other active materials can synergize the advantageous features between them, which enable specific capacitance. For example, Xiong *et al.* synthesized the hierarchical nanocomposites based on Co_3O_4 nanowire arrays and ultrathin PPy nanoflakes, such core/shell hybrid electrode exhibits the specific capacitance as high as 2017 F g^{-1} (areal capacitance of 4.90 F cm^{-2}) at a current density of 1 mA cm^{-2}.[141] Moreover, by forming a stable coating around the NCPs can provide effective strain accommodation during cycles, leading to a high cycling life. Thirdly, novel designs of NCPs-based supercapacitor showed improved stability.[1,12] Nanoarrays grown directly on current collectors possess better mechanical and structural stability compared to powders. For example, Xia *et al.* developed a highly stable electrode material based on core–shell structural PANI–RuO_2 nanofiber arrays. The ultrathin RuO_2 shell achieved by atomic layer deposition as a buffer layer not only effectively prevents the damage of the PANI structures during charge and discharge processes, but also facilitates the charge transfer and the electrolyte ion diffusion to the PANI electrodes. The symmetric pseudocapacitors of PANI/RuO_2 core–shell nanofiber arrays show an ultrahigh specific capacitance of 710 F g^{-1} at 5 mV s^{-1} (in full cell configuration), and enhanced cycling stability at very high current density ($\approx$88% capacitance retention after 10 000 cycles at 20 A g^{-1}).[142] As for the conductivity issue, an active material with a high conductivity will lower polarization and accelerate the reaction kinetics. Meanwhile, devices that use these unique nanostructured electrodes can have additional functionalities beyond energy storage, for instance, self-healing and shape memory.

In addition, advanced simulation and modeling studies are needed to uncover underlying electrochemical mechanisms in nanoscale to provide a deeper understanding of nanostructured CPs and their composites used in the supercapacitors. As a complementary strategy, state-of-the-art *in situ* microscopic and spectroscopic techniques are also needed to provide direct measurements for studying the nanoscale processes in energy storage.[143] The insights provided by these techniques will support optimizing the electrochemical properties of NCPs in revolutionary new nanostructured supercapacitor devices. In short, the goal for studying supercapacitor materials is to incorporate them into supercapacitor devices to apply in practical application. To further develop innovative solutions to present and future energy storage problems, research at the interface of polymer science and electrochemistry is crucial. Moreover, flexible and stretchable supercapacitors are also emerging.[143] Recent studies have shown that CP hydrogels possess excellent electrochemical activity, relatively high electrical conductivity, and adjustable mechanical properties, and have the potential to develop into next-generation wearable and portable electronics. Yu *et al.* presented an all-gel-state fibrous supercapacitor based on the 3D nanostructured PANI/graphene hydrogel with strong intermolecular interactions (Fig. 16a and b), and the device could power two LEDs while in the normal and curved states (Fig. 16c).[144] Such low-cost, lightweight, and high performance energy materials, which are prepared by scalable solution processing with earth-abundant and environment-friendly sources, will offer the feasible solution to create next generation of energy storage devices with superior power density and energy density.

4.4.3 Electrochromic devices. Developing high-performance electrochromic materials for energy-efficient displays has proven a challenging, but very important goal for global energy savings and sustainability.[145–152] Current, inorganic electrochromic materials (*e.g.*, WO_3 film) have been successfully commercialized, although their application has been limited by high production costs related to vacuum processing.[153,154] Recently, non-emissive electrochromic polymers (ECPs) received great attention recent decades due to their low-power consumption, facile color tunability through molecular design, application to flexible and rollable displays. Nanostructure-based CPs are rarely reported in the electrochromic field but it does not mean that they are unimportant.

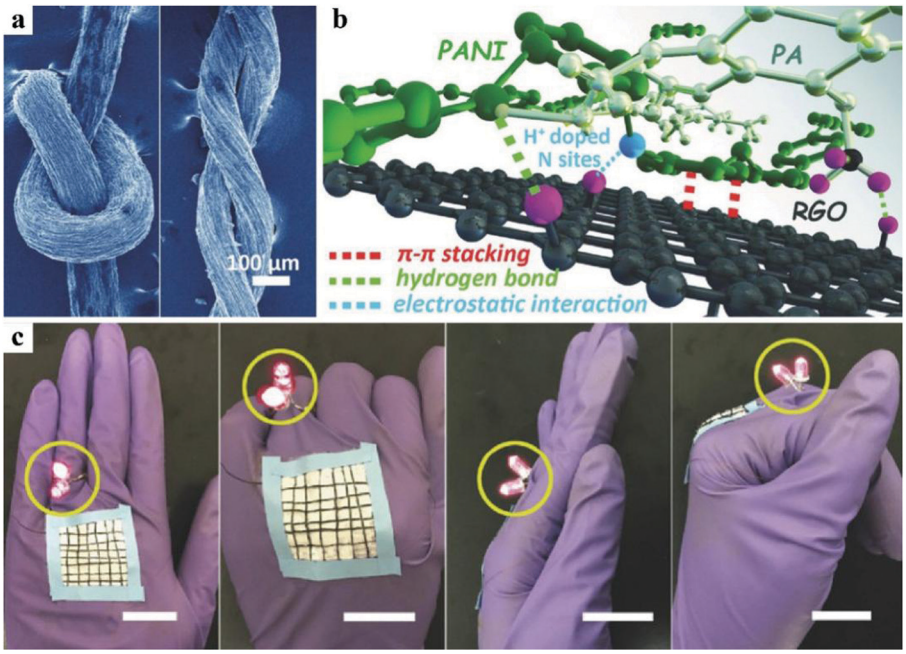

Fig. 16 (a) Morphologies of PANI/RGO fibers, (b) the interaction among PANI, PA, and RGO, (c) a demonstration of a fabricated yarn powering two LEDs in the normal and curved states (the scale bars are 2 cm). Reprinted with permission from ref. 144. Copyright 2018 Wiley-VCH.

Bulk electrochromic polymer films suffer from various shortcomings including slow color-switching rate, short color-duration, poor reversibility, and purity. In particular, the optical response caused by a chemical trigger is often diffusion limited, causing relatively slow response times. However, the optical response time of promising bulk CP films range from hundreds of milliseconds to seconds. In terms of shortening switching time (t_s), the simplest way is thinning the EC layer which would decrease the diffusion length of carriers to assist with the slow kinetics, but this would be accompanied with the loss of color contrast.[155] However, utilizing nanoscale materials with a large interface and small diffusion length would enhance the optical

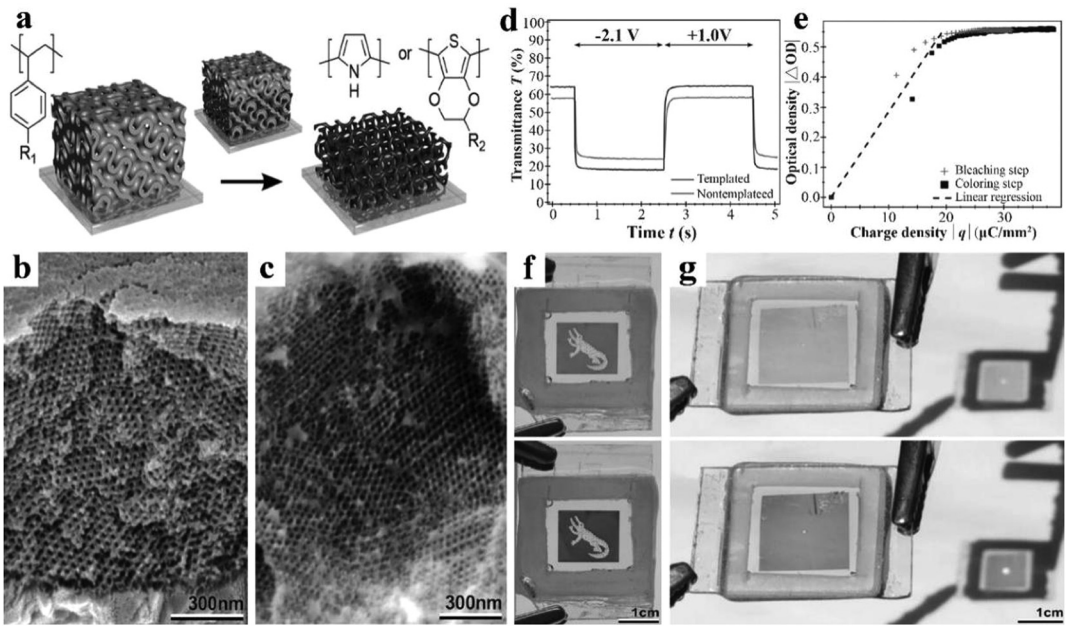

Fig. 17 (a) Schematic illustration of the gyroidal styrenic template, electropolymerization, and subsequent template dissolution yielding a freestanding conjugated polymer replica (R_1 = H, F and R_2 = H, CH_2OH). Cross-sectional SEM images of (b) free-standing, mesoporous PEDOT-MeOH and (c) PPy networks. (d) Time-resolved switching behavior of double-gyroid structured and nontemplated PEDOT-MeOH films. (e) Optical density *versus* charge density calculated from and the switching current. (f and g) The double-gyroid structured PEDOT-MeOH electrochromic devices. Reprinted with permission from ref. 156. Copyright 2015 Wiley-VCH.

contrast (ΔT) and t_s, respectively. Nanostructures can ensure fast ion/electron diffusion and larger active surface area, giving rise to improved optical contrast and fast switching time. For example, Steiner *et al.* reported a strategy to develop a high-performance electrochromic polymer by employing molecular template with gyroid morphology (Fig. 17a), and the resulting polymers with mesoporous structure (Fig. 17b and c). The assembled devices present excellent electrochromic performance including optimal coloration contrast of 48.5% and fast switching time of 23 and 14 ms for the coloring and bleaching process. (Fig. 17d and e)[156] Such nanostructure provide a short pathway for ionic diffusion, ensuring devices with fast switching rate under doping and dedoping processes. The electrochromic devices were shown in Fig. 17f and g.

Increasing research has been drawn onto the hybrid electrochromic materials based on NCPs and inorganic materials in recent years, mainly owing to their potential complementary advantages. But hybrid electrochromic films usually possess long ion diffusion distance, seriously limiting the long-term stability. NCPs with 1D nanostructure possess sufficient active sites on wide open surface area and shorten the diffusion path for ions, and its stability can be mainly attributed to structural fracture and particulate aggregation in long-term cycles. Thus, the development of high-performance hybrid electrochromic materials with good stability requires feasible strategy to design nanocomposites with short ion diffusion distance. Kateb *et al.* reported an ultrafast, high contrast and transparent electrochromic display by fabricating nanostructured electrode based on PEDOT and ZnO nanocomposites.[155] A device fabricated from such composites demonstrated ultrafast switching time of 2.2 ms (for both colored and de-colored states) and diffusion coefficient of 2.01×10^{-4} cm^2 s^{-1}, which is unmatched by bulky polymer materials. Moreover, the nanocomposite material showed excellent stability with the color contrast maintained even after tens of thousands of cycles. Such outstanding stability can be attributed to the ultrafast diffusion kinetic occurring in the electrochromic composite.

5. Summary and prospects

Commendable progress has been made on the synthesis, morphological and structural characterization, and properties for NCPs during the last few decades. As described in this review, recent advances in the synthetic technologies and morphologic control methods as well as their applications in optoelectronics, sensors, energy, and biomedical therapeutic have summarized. These widespread researches and applications arise from the attractive properties of NCPs, such as sufficiently high electrical conductivity, and biocompatibility. While current technologies have achieved diverse nanostructures, developing facile and efficient methods to synthesize the NCPs on a large scale with uniform, non-aggregating, and well-defined morphology and size is still under development. Moreover, to developing NCPs with tunable microstructures and controllable chemical/physical properties still remains an enduring challenge.

New challenges are arising from the rapidly developments in energy, electronic, optical and biological areas, which required NCPs with higher electronic conductivity and capacitive storage capacity, and broader optical absorption as well as good biological compatibility. Looking to future studies, developments should focuses on improving synthetic methods to accuracy control the morphology, optimizing the performance, and extending availability for more applications. For example, NCPs with single-crystal structure can present ultrahigh conductivity, thus should take an in-depth studying on the crystallography of CPs. With careful design a NCPs possessing high mechanical stability will continue to be crucial to the development of flexible, stretchable and wearable circuits. There is no doubt about CP nanocomposites can solve intrinsic problems of individual components and offer enhanced properties to expand potential applications. Thus a deep understanding on the interface effects between NCPs and other active materials such as carbons, metals, metal oxides, and polymers is vital for constructing suitable composites. In addition, advanced characterization tools need to be used to accurately depict NCPs system, such as the aggregation states of polymeric chains, the interactions between doping molecules and polymer backbones, mapping of dopant dispersion, and surface states between the gel matrix and incorporated functional materials. Finally, in order to accelerate the pace of developments, interdisciplinary integration is required, such as polymer physics, chemical science, device assembly and biological medicine.

Author contributions

Xue Y and Chen S proposed the topic and outline of this review article. Xue Y, Yu JR, and Xue ZX collected the related in-formation needed in writing the paper. Xue Y, Chen S, Yu JR, Bunes BR, Lu BY, Xu JK and Zang L wrote and modified the manuscript. All authors discussed and commented on the manuscript.

Conflicts of interest

There are no conflicts to declare.

Acknowledgements

We are grateful to the National Natural Science Foundation of China (No. 51963011 and 51763010), the Scholarship from China Scholarship Council (No. 201808360327), the Natural Science Foundation of Jiangxi Province (No. 20192BAB216012), and the Academic and Technical Leader Plan of Jiangxi Provincial Main Disciplines (No. 20194BCJ22013) for their financial support of this work.

References

1 F. Zhao, Y. Shi, L. J. Pan and G. H. Yu, *Acc. Chem. Res.*, 2017, **50**, 1734–1743.

2 A. J. Heeger, *Chem. Soc. Rev.*, 2010, **39**, 2354–2371.
3 S. Inal, J. Rivnay, A. O. Suiu, G. G. Malliaras and I. McCulloch, *Acc. Chem. Res.*, 2018, **51**, 1368–1376.
4 H. Yuk, B. Y. Lu and X. H. Zhao, *Chem. Soc. Rev.*, 2019, **48**, 1642–1667.
5 L. Zhang, W. Y. Du, A. Nautiyal, Z. Liu and X. Y. Zhang, *Sci. China Mater.*, 2018, **61**, 303–352.
6 M. Fahlman, S. Fabiano, V. Gueskine, D. Simon, M. Berggren and X. Crispin, *Nat. Rev. Mater.*, 2019, **4**, 627–650.
7 Y. Z. Long, M.-M. Li, C. Z. Gu, M. X. Wan, J. L. Duvail, Z. W. Liu and Z. Y. Fan, *Prog. Polym. Sci.*, 2011, **36**, 1415–1442.
8 T. L. Kelly and M. O. Wolf, *Chem. Soc. Rev.*, 2010, **39**, 1526–1535.
9 C. Mijangos, R. Hernández and J. Martin, *Prog. Polym. Sci.*, 2016, **54**, 148–182.
10 X. F. Lu, W. J. Zhang, C. Wang, T. C. Wen and Y. Wei, *Prog. Polym. Sci.*, 2011, **36**, 671–712.
11 S. Nardecchia, D. Carriazo, M. L. Ferrer, M. C. Gutierrez and F. D. Monte, *Chem. Soc. Rev.*, 2013, **42**, 794–830.
12 M. X. Wan, *Conducting polymer with micro and nanometer structure*, Springer, 2008, p. 307.
13 H. D. Yu, M. D. Regulacio, E. Ye and M. Y. Han, *Chem. Soc. Rev.*, 2013, **42**, 6006–6018.
14 D. C. Wu, F. Xu, B. Sun, R. W. Fu, H. K. He and K. Matyjaszewski, *Chem. Rev.*, 2012, **112**, 3959–4015.
15 R. B. Ambade, S. B. Ambade, N. K. Shrestha, R. R. Salunkhe, W. Lee, S. S. Bagde, J. H. Kim, F. J. Stadler, Y. Yamauchi and S. H. Lee, *J. Mater. Chem. A*, 2017, **5**, 172–180.
16 S. H. Mujawar, S. B. Ambade, T. Battumur, R. B. Ambade and S. H. Lee, *Electrochim. Acta*, 2011, **56**, 4462–4466.
17 M. Q. Xue, F. W. Li, D. Chen, Z. H. Yang, X. W. Wang and J. H. Ji, *Adv. Mater.*, 2016, **28**, 8067.
18 K. S. Jeng, C. W. Chu, C. L. Liu, W. M. Jean, H. L. Chen and J. T. Chen, *Macromol. Chem. Phys.*, 2018, **219**, 1800078.
19 Y. Choi, J. Lee, H. Ahn, J. Lee, H. C. Choi and M. J. Park, *Angew. Chem., Int. Ed.*, 2015, **54**, 10497–10501.
20 R. X. Yuan, H. Y. Wang, T. Ji, L. W. Mu, L. Chen, Y. J. Zhu and J. H. Zhu, *J. Mater. Chem. A*, 2015, **3**, 19299–19303.
21 Y. Ma, C. P. Hou, H. Zhang, M. T. Qiao, Y. H. Chen, H. P. Zhang, Q. Y. Zhang and Z. H. Guo, *J. Mater. Chem. A*, 2017, **5**, 14041–14052.
22 Y. Yang, D. Wang, Y. J. Wu, X. R. Tian, H. L. Qin, L. Hu, T. Zhang, W. H. Ni and J. Jin, *Macromol. Rapid Commun.*, 2016, **37**, 590–596.
23 X. F. Lu, C. Wang, F. Favier and N. Pinna, *Adv. Energy Mater.*, 2017, **7**, 1601301.
24 E. Sapountzi, M. Braiek, J. F. Chateaux, N. Jaffrezic-Renault and F. Lagarde, *Sensors*, 2017, **17**, 1887.
25 J. R. Cárdenas, M. G. O. de Franca, E. A. de Vasconcelos, W. M. de Azevedo and E. F. da Silva Jr, *J. Phys. D: Appl. Phys.*, 2007, **40**, 1068–1071.
26 T. S. Kang, S. W. Lee, J. Joo and J. Y. Lee, *Synth. Met.*, 2005, **153**, 61–64.
27 M. Mohamadali, S. Irani, M. Soleimani and S. Hosseinzadeh, *Polym. Adv. Technol.*, 2017, **28**, 1078–1087.
28 N. Radacsi, F. D. Campos, C. R. I. Chisholm and K. P. Giapis, *Nat. Commun.*, 2018, **9**, 4740.
29 M. J. T. Raaijmakers and N. E. Benes, *Prog. Polym. Sci.*, 2016, **63**, 86–142.
30 L. Güniat, P. Caroff and A. F. i Morral, *Chem. Rev.*, 2019, **119**, 8958–8971.
31 A. T. Lawal and G. G. Wallace, *Talanta*, 2014, **119**, 133–143.
32 L. M. Santino, S. Acharya and J. M. D'Arcy, *J. Mater. Chem. A*, 2017, **5**, 11772–11780.
33 B. Kolodziejczyk, O. Winther-Jensen, C. H. Ng, S. H. Lin, Q. L. Bao and B. Winther-Jensen, *Mater. Horiz.*, 2014, **1**, 452–460.
34 C. Debiemme-Chouvy, A. Fakhry and F. Pillier, *Electrochim. Acta*, 2018, **268**, 66–72.
35 A. Hajian, A. A. Rafati, A. Afraz and M. Najafi, *J. Electrochem. Soc.*, 2014, **161**, 196–200.
36 Y. J. Kim, H. T. Jung, C. W. Ahn and H. J. Jeon, *Adv. Mater. Interfaces*, 2017, **4**, 1700342.
37 W. I. Park, D. H. Kim, J. Jung, S. W. Hong, Z. Lin and M. Byun, *Adv. Mater. Technol.*, 2019, **4**, 1800554.
38 S. Islam, H. Bakhtiar, N. Bidin, A. A. Salim, S. Riaz, K. N. Abbas, L. P. Suan and S. Naseem, *J. Saudi Chem. Soc.*, 2018, **22**, 826–837.
39 A. A. Salim, H. Bakhtiar, N. Bidin and S. K. Ghoshal, *Opt. Mater.*, 2018, **85**, 100–105.
40 V. Amendola and M. Meneghetti, *Phys. Chem. Chem. Phys.*, 2013, **15**, 3027–3046.
41 D. S. Zhang, J. Liu and C. H. Liang, *Sci. China: Phys., Mech. Astron.*, 2017, **60**, 074201.
42 C. A. Amarnath and S. N. Sawant, *Polymer*, 2016, **87**, 129–137.
43 Y. Wang, S. Q. Xu, W. F. Liu, H. Cheng, S. Y. Chen, X. Q. Liu, J. Y. Liu, Q. D. Tai and C. L. Hu, *Electrochim. Acta*, 2017, **254**, 25–35.
44 M. Yang, L. J. Cao and L. Tan, *Colloids Surf., A*, 2014, **441**, 678–684.
45 M. J. Kim, Y. D. Liu and H. J. Choi, *Chem. Eng. J.*, 2014, **235**, 186–190.
46 C. Y. Gao, L. Y. Meng, S. H. Piao and H. J. Choi, *Polymer*, 2018, **140**, 80–88.
47 F. X. Yin, D. R. Wang and Z. Zhang, *Mater. Lett.*, 2017, **207**, 225–229.
48 L. Güniat, P. Caroff and A. F. Morral, *Chem. Rev.*, 2019, **119**, 8958–8971.
49 Y. B. Li, J. Zhai, S. C. Hu, C. L. Zhang, J. Cui, M. Q. Zheng and Y. P. Yuan, *Colloid Polym. Sci.*, 2015, **293**, 329–332.
50 J. Zhao, D. X. Tan and G. M. Chen, *J. Mater. Chem. C*, 2017, **5**, 47–53.
51 B. Cho, K. S. Park, J. Baek, H. S. Oh, Y.-E. K. Lee and M. M. Sung, *Nano Lett.*, 2014, **14**, 3321–3327.
52 S. Pan, M. Zhu, L. He, H. Zhang, F. Qiu, Z. Lin and J. Peng, *Macromol. Rapid Commun.*, 2018, **39**, 1800048.
53 S. H. Lee, J. Bae, S. W. Lee and J.-W. Jang, *Nanoscale*, 2015, **7**, 17328–17337.
54 Z. D. Kojabad and S. A. Shojaosadati, *Mater. Des.*, 2016, **96**, 378–384.

55 F. Estrany, A. Calvet, L. J. del Valle, J. Puiggalí and C. Alemán, *Polym. Chem.*, 2016, **7**, 3540–3550.
56 S. H. Pang, W. L. Chen, Z. W. Yang, Z. Liu, X. Fan and D. Fang, *Polymers*, 2017, **9**, 510.
57 P. Olejnik, M. Gniadek, L. Echegoyen and M. E. Plonska-Brzezinska, *Polymers*, 2018, **10**, 1408.
58 F. Bonaccorso, L. Colombo, G. Yu, M. Stoller, V. Tozzini, A. C. Ferrari, R. S. Ruoff and V. Pellegrini, *Science*, 2015, **347**, 1246501.
59 Y. J. Yang, S. B. Li, W. Y. Yang, W. T. Yuan, J. H. Xu and Y. D. Jiang, *ACS Appl. Mater. Interfaces*, 2014, **6**, 13807–13814.
60 S. Liu, Y. H. Ma, R. Q. Zhang and X. L. Luo, *ChemElectroChem*, 2016, **3**, 1799–1804.
61 S. H. Liu, F. X. Wang, R. H. Dong, T. Zhao, J. Zhang, X. D. Zhang, Y. Y. Mai and X. L. Feng, *Adv. Mater.*, 2016, **28**, 8365–8370.
62 X. W. Yang, Z. X. Lin, J. X. Zheng, Y. J. Huang, B. Chen, Y. Y. Mai and X. L. Feng, *Nanoscale*, 2016, **8**, 8650–8657.
63 B. Y. Lu, H. Yuk, S. T. Lin, N. N. Jian, K. Qu, J. K. Xu and X. H. Zhao, *Nat. Commun.*, 2019, **10**, 1043.
64 Y. Shi, L. J. Pan, B. R. Liu, Y. Q. Wang, Y. Cui, Z. N. Bao and G. H. Yu, *J. Mater. Chem. A*, 2014, **2**, 6086–6091.
65 V. R. Feig, H. Tran, M. Lee and Z. N. Bao, *Nat. Commun.*, 2018, **9**, 2740.
66 Y. Zhao, B. R. Liu, L. J. Pan and G. H. Yu, *Energy Environ. Sci.*, 2013, **6**, 2856–2870.
67 L. B. Jiang, X. Z. Yuan, J. Liang, J. Zhang, H. Wang and G. M. Zeng, *J. Power Sources*, 2016, **331**, 408–425.
68 J. W. Park, W. Na and J. Jang, *J. Mater. Chem. A*, 2016, **4**, 8263–8271.
69 J. W. Li, S. J. Yoon, B.-Y. Hsieh, W. Y. Tai, M. O'Donnell and X. H. Gao, *Nano Lett.*, 2015, **15**, 8217–8222.
70 K. X. Zhang, J. K. Xu, X. M. Duan, L. M. Lu, D. F. Hu, L. Zhang, T. Nie and K. B. Brown, *Electrochim. Acta*, 2014, **137**, 518–525.
71 Q. Y. Zhou, Y. L. Zhou, M. Bao and X. Y. Ni, *Appl. Surf. Sci.*, 2019, **487**, 236–243.
72 X. F. Lu, X. Y. Chen, W. Zhou, Y. X. Tong and G. R. Li, *ACS Appl. Mater. Interfaces*, 2015, **7**, 14843–14850.
73 R. B. Ambade, S. B. Ambade, N. K. Shrestha, R. R. Salunkhe, W. Lee, S. S. Bagde, J. H. Kim, F. J. Stadler, Y. Yamauchi and S.-H. Lee, *J. Mater. Chem. A*, 2017, **5**, 172–180.
74 L. B. Jiang, X. Z. Yuan, J. Liang, J. Zhang, H. Wang and G. M. Zeng, *J. Power Sources*, 2016, **331**, 408–425.
75 R. A. Petros and J. M. DeSimone, *Nat. Rev. Drug Discovery*, 2010, **9**, 615–627.
76 D. Uppalapati, B. J. Boyd, S. Garg, J. Travas-Sejdic and D. Svirskis, *Biomaterials*, 2016, **111**, 149–162.
77 Y. G. Shi, M. Y. Liu, F. J. Deng, G. J. Zeng, Q. Wan, X. Y. Zhang and Y. Wei, *J. Mater. Chem. B*, 2017, **5**, 194–206.
78 X. J. Song, C. Liang, H. Gong, Q. Chen, C. Wang and Z. Liu, *Small*, 2015, **32**, 3932–3941.
79 H. Chong, C. Y. Nie, C. L. Zhu, Q. Yang, L. B. Liu, F. T. Lv and S. Wang, *Langmuir*, 2012, **28**, 2091–2098.
80 C. L. Zhu, L. B. Liu, Q. Yang, F. T. Lv and S. Wang, *Chem. Rev.*, 2012, **112**, 4687–4735.
81 D. F. Xu, L. Fan, L. F. Gao, Y. Xiong, Y. F. Wang, Q. F. Ye, A. X. Yu, H. L. Dai, Y. X. Yin, J. Cai and L. N. Zhang, *ACS Appl. Mater. Interfaces*, 2016, **827**, 17090–17097.
82 Z. Q. Shi, H. C. Gao, J. Feng, B. B. Ding, X. D. Cao, S. Kuga, Y. J. Wang, L. N. Zhang and J. Cai, *Angew. Chem., Int. Ed.*, 2014, **53**, 5380–5384.
83 W. H. Zhou, L. Lu, D. F. Chen, Z. G. Wang, J. X. Zhai, R. X. Wang, G. X. Tan, J. P. Mao, P. Yu and C. Y. Ning, *J. Mater. Chem. B*, 2018, **6**, 3128–3135.
84 E. Shamaeli and N. Alizadeh, *Int. J. Pharm.*, 2014, **472**, 327–338.
85 M. A. C. Stuart, W. T. S. Huck, J. Genzer, M. Müller, C. Ober, M. Stamm, G. B. Sukhorukov, I. Szleifer, V. V. Tsukruk, M. Urban, F. Winnik, S. Zauscher, I. Luzinov and S. Minko, *Nat. Mater.*, 2010, **9**, 101–113.
86 J. N. Anker, W. P. Hall, O. Lyandres, N. C. Shah, J. Zhao and R. P. V. Duyne, *Nat. Mater.*, 2008, **7**, 442–453.
87 S. Iqbal and S. Ahmad, *J. Ind. Eng. Chem.*, 2018, **60**, 53–84.
88 M. H. Naveen, N. G. Gurudatt and Y. B. Shim, *Appl. Mater. Today*, 2017, **9**, 419–433.
89 D. G. Prajapati and B. Kandasubramanian, *Macromol. Chem. Phys.*, 2019, **220**, 1800561.
90 G. X. Wang, A. Morrin, M. R. Li, N. Z. Liu and X. L. Luo, *J. Mater. Chem. B*, 2018, **6**, 4173–4190.
91 H. Y. Jia, J. K. Xu, L. M. Lu, Y. F. Yu, Y. X. Zuo, Q. Y. Tian and P. Li, *Sens. Actuators, B*, 2018, **260**, 990–997.
92 T. T. Yang, Y. S. Gao, Z. Liu, J. K. Xu, L. M. Lu and Y. F. Yu, *Sens. Actuators, B*, 2017, **239**, 76–84.
93 K. X. Zhang, J. K. Xu, X. M. Duan, L. M. Lu, D. F. Hu, L. Zhang, T. Nie and K. B. Brown, *Electrochim. Acta*, 2014, **137**, 518–525.
94 Y. S. Gao, J. K. Xu, L. M. Lu, L. P. Wu, K. X. Zhang, T. Nie, X. F. Zhu and Y. Wu, *Biosens. Bioelectron.*, 2014, **62**, 261–267.
95 T. T. Tung, D. losic, S. J. Park, J.-F. Feller and T. Y. Kim, *Int. J. Nanomed.*, 2015, **10**, 203–214.
96 P. Liu, Y. S. Zhu, S. H. Lee and M. Yun, *Biomed. Microdevices*, 2016, **18**, 113.
97 X. Y. Xue, Y. M. Fu, Q. Wang, L. L. Xing and Y. Zhang, *Adv. Funct. Mater.*, 2016, **26**, 3128–3138.
98 T. Someya and M. Amagai, *Nat. Biotechnol.*, 2019, **37**, 382–388.
99 C. K. Cui, Y. C. Du, T. H. Li, X. Y. Zheng, X. H. Wang, X. J. Han and P. Xu, *J. Phys. Chem. B*, 2012, **116**, 9523–9531.
100 Y. Wang, Y. C. Du, P. Xu, R. Qiang and X. J. Han, *Polymers*, 2017, **9**, 29.
101 L. Kong, X. W. Yin, X. Y. Yuan, Y. J. Zhang, X. M. Liu, L. F. Cheng and L. T. Zhang, *Carbon*, 2014, **73**, 185–193.
102 A. Pron and P. Rannou, *Prog. Polym. Sci.*, 2002, **27**, 135–190.
103 P. Chandrasekhar and K. Naishadham, *Synth. Met.*, 1999, **105**, 115–120.
104 R. Pang, X. J. Hu, S. Y. Zhou, C. H. Sun, J. Yan, X. M. Sun, S. Z. Xiao and P. Chen, *Chem. Commun.*, 2014, **50**, 12493–12496.
105 J. Liu, Y. H. Jia, Q. L. Jiang, F. X. Jiang, C. C. Li, X. D. Wang, P. Liu, P. P. Liu, F. Hu, Y. K. Du and J. K. Xu, *ACS Appl. Mater. Interfaces*, 2018, **1050**, 44033–44040.

106 H. Shi, C. C. Liu, Q. L. Jiang and J. K. Xu, *Adv. Electron. Mater.*, 2015, 1500017.
107 X. D. Wang, F. L. Meng, T. Z. Wang, C. C. Li, H. T. Tang, Z. M. Gao, S. Li, F. X. Jiang and J. K. Xu, *J. Alloys Compd.*, 2018, **734**, 121–129.
108 E. D. Liu, C. C. Liu, Z. Y. Zhu, J. K. Xu, F. X. Jiang, T. Z. Wang and C. C. Li, *J. Compos. Mater.*, 2017, **52**, 621–627.
109 H. Shi, C. C. Liu, Q. L. Jiang, J. K. Xu, B. Y. Lu, F. X. Jiang and Z. Y. Zhu, *Nanotechnology*, 2015, **26**, 245401.
110 C. C. Li, F. X. Jiang, C. C. Liu, P. P. Liu and J. K. Xu, *Appl. Mater. Today*, 2019, **15**, 543–557.
111 A. S. Arico, P. Bruce, B. Scrosati, J. M. Tarascon and W. V. Schalkwijk, *Nat. Mater.*, 2005, **4**, 366–377.
112 W. Q. Zhou, X. M. Ma, F. X. Jiang and J. K. Xu, *Electrochim. Acta*, 2014, **138**, 270–277.
113 D. Z. Mo, W. Q. Zhou, X. M. Ma and J. K. Xu, *Electrochim. Acta*, 2015, **155**, 29–37.
114 X. M. Ma, W. Q. Zhou, D. Z. Mo, J. Hou and J. K. Xu, *Electrochim. Acta*, 2015, **176**, 1302–1312.
115 H. T. Liu, W. Q. Zhou, X. M. Ma, S. Chen, S. L. Ming, K. W. Lin, B. Y. Lu and J. K. Xu, *Electrochim. Acta*, 2016, **220**, 340–346.
116 M. Bharti, A. Singh, S. Samanta and D. K. Aswal, *Prog. Mater. Sci.*, 2018, **93**, 270–310.
117 J. Kim, J.-H. Bahk, J. Hwang, H. Kim, H. Park and W. Kim, *Phys. Status Solidi RRL*, 2013, 1–14.
118 C. Gayner and K. K. Kar, *Prog. Mater. Sci.*, 2016, **83**, 330–382.
119 K. W. Shah, S.-X. Wang, D. X. Y. Soo and J. W. Xu, *Appl. Sci.*, 2019, **9**, 1422.
120 L. D. Zhao, S.-H. Lo, Y. S. Zhang, H. Sun, G. J. Tan, C. Uher, C. Wolverton, V. P. Dravid and M. G. Kanatzidis, *Nature*, 2014, **508**, 373–377.
121 G.-H. Kim, L. Shao, K. Zhang and K. P. Pipe, *Nat. Mater.*, 2013, **12**, 719–723.
122 F. X. Jiang, J. K. Xu, B. Y. Lu, Y. Xie, R. J. Huang and L. F. Li, *Chin. Phys. Lett.*, 2008, **25**, 2202–2205.
123 A. García-Barberá, M. Culebras, S. Roig-Sánchez, C. M. Gómez and A. Cantarero, *Synth. Met.*, 2016, **220**, 208–212.
124 D. K. Taggart, Y. Yang, S.-C. Kung, T. M. McIntire and R. M. Penner, *Nano Lett.*, 2010, **11**, 125–131.
125 X. Hu, G. Chen, X. Wang and H. Wang, *J. Mater. Chem. A*, 2015, **3**, 20896–20902.
126 J. Zhang, K. Zhang, F. Xu, S. Wang and Y. Qiu, *Composites, Part B*, 2018, **136**, 234–240.
127 B. Endrődi, J. Mellar, Z. Gingl, C. Visy and C. Janáky, *RSC Adv.*, 2014, **4**, 55328–55333.
128 S. Hiura, N. Okada, J. Wakui, H. Narita, S. Kanehashi and T. Shimomura, *Materials*, 2017, **10**, 468.
129 J. Wu, Y. Sun, W.-B. Pei, L. Huang, W. Xu and Q. Zhang, *Synth. Met.*, 2014, **196**, 173–177.
130 Y. Du, H. Niu, J. Li, Y. Dou, S. Shen, R. Jia and J. Xu, *Polymers*, 2018, **10**, 1143.
131 L. Liang, G. Chen and C.-Y. Guo, *Mater. Chem. Front.*, 2017, **1**, 380–386.
132 Y. Sun, Z. Wei, W. Xu and D. Zhu, *Synth. Met.*, 2010, **160**, 2371–2376.
133 J. Wu, Y. Sun, W. Xu and Q. Zhang, *Synth. Met.*, 2014, **189**, 177–182.
134 M. E. Abdelhamid, A. P. O'Mullane and G. A. Snook, *RSC Adv.*, 2015, **5**, 11611–11626.
135 S. Ghosh, T. Maiyalagan and R. N. Basu, *Nanoscale*, 2016, **8**, 6921–6947.
136 I. Shown, A. Ganguly, L. C. Chen and K. H. Chen, *Energy Sci. Eng.*, 2015, **3**, 2–26.
137 Y. Huang, H. F. Li, Z. F. Wang, M. S. Zhu, Z. X. Pei, Q. Xue, Y. Huang and C. Y. Zhi, *Nano Energy*, 2016, **22**, 422–438.
138 J. F. Wang, J. R. Wang, Z. Kong, K. L. Lv, C. Teng and Y. Zhu, *Adv. Mater.*, 2017, **29**, 1703044.
139 Z. T. Zhang, M. Liao, H. Q. Lou, Y. J. Hu, X. M. Sun and H. S. Peng, *Adv. Mater.*, 2018, **30**, 1704261.
140 Y. G. Wang, Y. F. Song and Y. Y. Xia, *Chem. Soc. Rev.*, 2016, **45**, 5925–5950.
141 W. Xiong, X. X. Pan, Y. Li, X. M. Chen, Y. F. Zhu, M. Yang and Y. Zhang, *Mater. Lett.*, 2015, **157**, 23–26.
142 C. Xia, W. Chen, X. B. Wang, M. N. Hedhili, N. N. Wei and H. N. Alshareef, *Adv. Energy Mater.*, 2015, 1401805.
143 D. P. Dubal, N. R. Chodankar, D. H. Kim and P. Gomez-Romero, *Chem. Soc. Rev.*, 2018, **47**, 2065–2129.
144 P. P. Li, Z. Y. Jin, L. L. Peng, F. Zhao, D. Xiao, Y. Jin and G. H. Yu, *Adv. Mater.*, 2018, **30**, 1800124.
145 Y. Xue, Z. X. Xue, W. W. Zhang, W. N. Zhang, S. Chen, K. W. Lin and J. K. Xu, *J. Electroanal. Chem.*, 2019, **834**, 150–160.
146 Y. Xue, Z. X. Xue, W. W. Zhang, W. N. Zhang, S. Chen, K. W. Lin and J. K. Xu, *J. Polym. Sci., Part A: Polym. Chem.*, 2019, **57**, 1041–1048.
147 Y. Xue, Z. X. Xue, W. W. Zhang, W. N. Zhang, S. Chen, K. W. Lin and J. K. Xu, *Polymer*, 2018, **159**, 150–156.
148 N. N. Jian, H. Gu, S. M. Zhang, H. T. Liu, K. Qu, S. Chen, X. M. Liu, Y. F. He, G. F. Niu, S. Y. Tai, J. Wang, B. Y. Lu, J. K. Xu and Y. Yu, *Electrochim. Acta*, 2018, **266**, 263–275.
149 W. W. Zhang, W. N. Zhang, Z. X. Xue, Y. Xue, N. N. Jian, K. Qu, H. Gu, S. Chen and J. K. Xu, *Electrochim. Acta*, 2018, **278**, 313–323.
150 B. Y. Lu, S. J. Zhen, S. M. Zhang, J. K. Xu and G. Q. Zhao, *Polym. Chem.*, 2014, **5**, 4896–4908.
151 S. L. Ming, S. J. Zhen, K. W. Lin, L. Zhao, J. K. Xu and B. Y. Lu, *ACS Appl. Mater. Interfaces*, 2015, **7**, 11089–11098.
152 P. M. Beaujuge and J. R. Reynolds, *Chem. Rev.*, 2010, **110**, 268–320.
153 X. Yu, T. J. Marks and A. Facchetti, *Nat. Mater.*, 2016, **15**, 383–396.
154 N. E. Dov, S. Shankar, D. Cohen, T. Bendikov, K. Rechav, L. J. W. Shimon, M. Lahav and M. E. V. D. Boom, *J. Am. Chem. Soc.*, 2017, **139**, 11471–11481.
155 M. Kateb, S. Safarian and M. Kolahdouz, *Sol. Energy Mater. Sol. Cells*, 2016, **145**, 200–205.
156 R. Dehmel, A. Nicolas, M. R. J. Scherer and U. Steiner, *Adv. Funct. Mater.*, 2015, **25**, 6900–6905.